TISSUE DAMAGE SIGNALING IS ESSENTIAL FOR PROTECTIVE NEUTROPHIL RESPONSES TO MICROBIAL INFECTION IN ZEBRAFISH (*Danio rerio*)

A Dissertation

Presented to the Faculty of the Weill Cornell Graduate School

of Medical Sciences

in Partial Fulfillment of the Requirements for the Degree of

Doctor of Philosophy

by

Cong Huang

May 2018

TISSUE DAMAGE SIGNALING IS ESSENTIAL FOR PROTECTIVE NEUTROPHIL RESPONSES TO MICROBIAL INFECTION IN ZEBRAFISH

Cong Huang, Ph.D.

Cornell University 2018

Inflammation is an important biological response of body tissues to harmful stimuli. It is essential for the host to clear invading pathogens, cell debris and to initiate tissue regeneration. However, when deregulated, it can be deleterious to the host. Tissue damage-induced neutrophil infiltration, in the absence of bacterial infection, is documented to adversely affect the resolution of numerous diseases including ischemia, asthma, gout, cancer and others. It is of great clinical interest to interrogate the mechanism and the potential selective advantages, if any, of such deleterious response. Zebrafish has many advantages in studying inflammatory responses such as its conserved innate immune system compared to mammals, availability of large batches of embryos, and the transparency of zebrafish larvae which is ideal for intravital imaging. In this study, we show that selective inhibition of tissue damage-induced inflammation upon *Pseudomonas aeruginosa* (PA) infection abrogates neutrophil chemotaxis and reduces survival of infected zebrafish. Such result is achieved, at least in part, through the suppression of cytosolic phospholipase A2 ($cPla_2$), which mechanochemically integrates tissue damage- and microbe-derived cues. Thus, tissue damage-, but not microbe-, derived signals are sufficient for triggering neutrophil responses, and are essential for protecting zebrafish against infection.

BIOGRAPHICAL SKETCH

Cong Huang was born in Dingzhou, Hebei Province, China in 1989. He attended Liqingu Primary School in 1996. In 2001, Cong attended Beihuan Road Middle School till 2003. After that, he went on to Dingzhou No.1 High School from 2003 to 2007. Cong matriculated at College of Life Sciences of Nankai University, Tianjin, China, where he majored in Biological Sciences. Cong conducted his undergraduate thesis research in the lab of Dr. Zihe Rao in the Department of Structural Biology. After graduation, he worked as a research technician in the same lab for a year. In 2012, Cong started the doctoral program at Weill Cornell Graduate School of Medical Sciences of Cornell University. He joined the laboratory of Dr. Philipp Niethammer in the Cell Biology Department at Memorial Sloan Kettering Cancer Center in 2013, where he conducted his doctoral dissertation on the protective role of tissue damage signaling during microbial infection in zebrafish.

For my parents and my wife.

ACKNOWLEDGEMENTS

I would like to express my immense gratitude to my mentor, Dr. Philipp Niethammer, for his invaluable guidance throughout my journey of Ph.D.. I deeply appreciate for the opportunity to work on my thesis project as well as the freedom to explore my scientific interests. Philipp's dedication and passion to always chase the frontiers of science set a great example for what a true scientist should be. His expertise in the field has been the indispensible support for every step of my research and helped me push through the obstacles. Without him, I would not be able to grow and develop as a scientist.

I would also like extend my gratitude to my Thesis Committee members, Dr. Michael Overholtzer and Dr. Morgan Huse, for their valuable advice and brainstorming during every annual meeting; Dr. Meng-Fu Bryan Tsou, for agreeing to be the chairperson of my Dissertation Committee.

I am extremely grateful to every current and former members of the Niethammer lab. I would like to thank Dr. Will Gault for the mentorship during my rotation. I learned my first microscopy skills from Will and realized how big the biological world can be behind that little lens. I am also thankful to Dr. Balázs Enyedi. I could not remember how many valuable discussions that I had with him. Balázs was always helpful, patient, and smiling. I really learned a lot from him, both for science and life. I would also like to thank Mark Jelcic, Michelina Stoddard, Gary Gerlach, and King Lam Hui,

for numerous suggestions about my project and English learning. They made the lab a lovely place to be.

I am also grateful for the Cell Biology branch of MSKCC, especially the Overholtzer lab, the Haynes lab, the Foley lab, and the Jiang lab, for their kindness of sharing research materials and instruments. Additionally, I thank Dr. Joao Xavier, for the kind gift of bacteria strains.

I would like to thank all my graduate school classmates and friends for making graduate school such a pleasant journey. I also want to thank the people who helped me to adjust the school life in the United States: Andrew Koff, Kirk Deitsch, Stephen Long, Scott Keeney, Rosalia Mora, Denise Jenkins.

I would like to thank my parents for their unconditional love and support throughout my life.

Finally, I want to thank my wife, Xiaojing Mu, for all the happinesses, tears, and supports in the last six years. I would not finish my Ph.D. odyssey without her.

TABLE OF CONTENTS

LIST OF FIGURES

Chapter I

Chapter II

Chapter IV

LIST OF TABLES

Chapter I

Chapter IV

Chapter V

Chapter 1: Introduction

Section 1: Innate immune system

1.1 Overview of inflammatory responses

Inflammation is the immediate response of the host to tissue or cell damage caused by noxious instigators. Such instigators can come from microbial infection or tissue injury (Medzhitov, 2008). The pattern-recognition receptors (PRRs) presented on the outside of or within tissue resident leukocytes (such as macrophages and mast cells) and other cell types can recognize those instigators, which leads to the production of proinflammatory mediators such as chemokines, cytokines, and histamine (Areschoug and Gordon, 2008). Those mediators dilate the endothelium of the local vessels and cause neutrophil extravasation (Newton and Dixit, 2012). Once arriving at infected or damaged tissue, neutrophils are activated either directly via contact with the pathogen or indirectly by secreted cytokines from tissue-resident immune cells. Upon activation, neutrophils will eliminate the microbial or host targets through either phagocytosis or the secretion of toxic content, such as reactive oxygen species (ROS) and elastase, from their granules (Nathan, 2002, 2006).

Once the danger is eliminated, the inflammatory response will enter the resolution phase. Macrophages will switch lipid mediator production from pro-inflammatory to anti-inflammatory products, such as lipoxins, resolvins and protectins. Those anti-

inflammatory mediators inhibit recruitment of neutrophils and initiate tissue repair by attracting monocytes (Serhan, 2007; Serhan and Savill, 2005).

1.2 Triggers of inflammatory responses

Inflammation can be triggered by numerous tissue damage- or microbe-derived insults. Such instigators can be either exogenous or endogenous.

One classic exogenous stimulus is microbial infection. Upon infection, pathogen-associated molecular patterns (PAMPs), which represent a group of conserved microbe-specific molecules including lipopolysaccharide (LPS), flagellin, etc., will be released into the host. PAMPs can be recognized directly by PRRs of the host cells. For example, LPS, a common endotoxin of Gram-negative bacteria, can be recognized by Toll-like receptor 4 (TLR4) (Akira and Takeda, 2004; Chow et al., 1999; Park and Lee, 2013). Other type of PAMPs, such as microbial virulence factors, can be recognized indirectly through their damaging activity. For example, the NACHT-, leucine-rich repeat- and pyrin-domain-containing protein (NALP3) inflammasome detects the bacterial pore-forming exotoxins, such as nigericin, by monitoring K^+ efflux as indication for a damaged plasma membrane (Mariathasan et al., 2006).

Exogenous stimuli can also be non-microbial. Those sterile particles include crystals, minerals and protein aggregates (Rock et al., 2010). For example, patients with too much uric acid in their blood (hyperuricemia) crystallize monosodium urate (MSU) in their joint, which can trigger acute inflammatory responses. The recurrence of such

inflammatory response can cause joint damage and eventually lead to gout (Chen et al., 2006; Martinon et al., 2006).

Endogenous stimuli are produced by stressed or damaged tissues. They comprise the cellular molecules which are usually sequestered within intact cells, such as nuclear and cytoplasmic proteins. Those damage-associated molecular patterns (DAMPs) can be recognized by specialized receptors including PRRs. For example, extracellular high-mobility group box 1 protein (HMGB1) can be sensed by the advanced glycation end-product-specific receptor (RAGE) and thus triggers the downstream inflammatory response (Kokkola et al., 2005).

1.3 Sensors and pathways of inflammatory response

PRRs are the major receptors which recognize and response to PAMPs and DAMPs. PRRs include several receptor families, including Toll-like receptors (TLRs), NOD-like receptors (NLRs), C-type lectin receptors (CLRs), Scavenger receptors (SRs) and β_2-integrins. Based on their functions, PRRs can be divided into two categories: some PRRs, including TLRs and NLRs, are involved in signaling which leads to downstream inflammatory response and cellular activation; while other PRRs, such as scavenger receptors, mediate direct phagocytic uptake of microbial products (Areschoug and Gordon, 2008).

Here I mainly focus on inflammatory signaling related PRRs.

1.3.1 Toll like receptors (TLRs)

TLRs are type I membrane proteins containing the leucine-rich repeat (LRR), which is responsible for PAMP and DAMP recognition, and cytoplasmic Toll/interleukin(IL) 1 receptor (TIR) domain, which serves as docking site for downstream TIR-containing adaptor proteins (Newton and Dixit, 2012).

To date, 10 human TLRs have been identified. They are expressed in antigen-presenting cells (APCs) as well as other cell types such as epithelial cells (Mogensen, 2009). Based on cellular localization, TLRs can be divided into two groups: TLR1, TLR2, TLR4, TLR5, TLR6 and TLR10 are localized at cell surface, while TLR3, TLR7, TLR8, and TLR9 are localized in intracellular space (Kawasaki and Kawai, 2014). Each TLR has different specificity for a subset of molecules. For example, TLR3 recognizes double-stranded RNA (dsRNA) of virus (Alexopoulou et al., 2001), TLR4 recognize lipopolysaccharide (LPS) of Gram-negative bacteria (Chow et al., 1999), TLR5 recognizes bacteria flagellin (Hayashi et al., 2001), and TLR7 recognizes single-stranded RNA (ssRNA) from viruses (Mancuso et al., 2009).

Upon PAMP- and DAMP-detection, TLRs recruit TIR-containing adaptor proteins. MyD88 (myeloid differentiation primary-response gene 88) is the universal adaptor protein for all TLR signaling except TLR3 (Kawai and Akira, 2007). The engagement between TLR and MyD88 induces the autophosphorylation of IL-1R-associated kinases (IRAK), especially IRAK1 and IRAK4 (Kollewe et al., 2004). IRAK1 then interacts with TRAF6 (tumor necrosis factors (TNF) receptor-associated factor 6), an

E3 ligase. Together with UBC13 (ubiquitin-conjugating enzyme E2 N) and UEV1A (ubiquitin-conjugating enzyme E2 variant 1A), the ubiquitin-conjugating enzymes, TRAF6 forms a complex which promotes the synthesis of K63 polyubiquitin chains (Chen, 2012). Transforming growth factor β-activated kinase 1 (TAK1) is then activated and triggers the two downstream pathways: NF-κB (nuclear factor kappa-light-chain-enhancer of activated B cells) and MAPK (mitogen-activated protein kinases). NF-κB regulates the transcription of various proinflammatory genes, while MAP kinases phosphorylate and activate AP-1 (activator protein 1) transcription factors (Ajibade et al., 2013; Kawasaki and Kawai, 2014) (Figure 1.1).

TLRs can also trigger TRIF (TIR-domain-containing adaptor protein inducing interferon-β)-dependent pathway. TRAF3 and TRAF6 are the main downstream proteins of TRIF. TRAF3 is known to activate IKK (inhibitor of kappa B kinase)-related kinase, TBK1 (TANK (TRAF family member-associated NF-κB activator)-binding kinase 1) and IKKi, which leads to the phosphorylation of IRF3 (interferon regulatory transcription factor 3). IRF3 then induces the production of IFNβ (Sharma et al., 2003). TRAF6, on the other hand, interacts with RIP1 (receptor-interacting serine/threonine-protein kinase 1) kinase, which recruits TAK1 and eventually leads to the activation of NF-κB and MAPK pathways as mentioned above (Sato et al., 2003) (Figure 1.1).

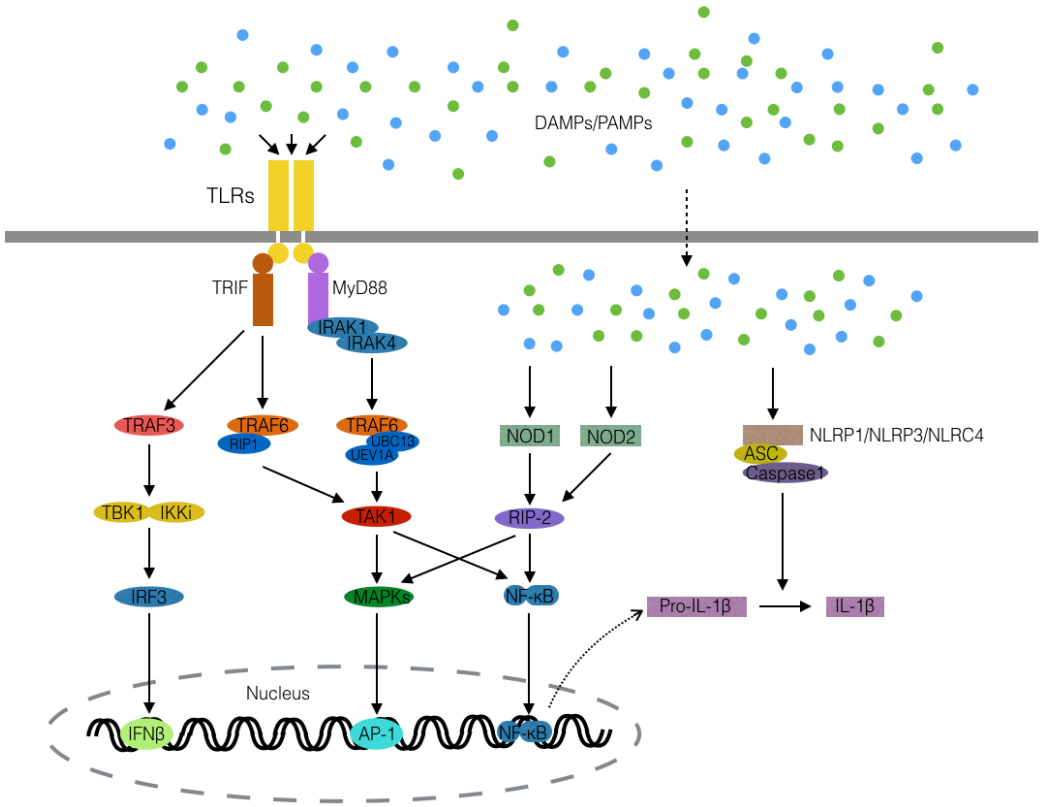

Figure 1.1 TLR and NLR signaling pathways.

1.3.2 NOD-like receptors (NLRs)

NLRs are intracellular proteins that share a central nucleotide-binding domain (NACHT domain) and a LRR domain. In human, NLR family contains 23 cytosolic proteins (Franchi et al., 2008).

Upon sensing different bacterial peptidoglycan components, NOD1 and NOD2 interact with caspase-recruiting domain (CARD)-containing kinase RIP-2 to activate MAPK and NF-κB signaling pathways (Park et al., 2007).

PAMPs and DAMPs can also trigger other NLRs, including NLRP1, NLRP3 and NLRC4, to form the inflammasome by recruiting the CARD- and PYRIN-domain containing adaptor ASC. ASC will then bind the CARD domain and facilitate the autocatalytic activation of aspartate-specific cysteine protease caspase-1, which cleaves pro-IL1β and pro-IL18 to their mature forms (Mariathasan et al., 2004) (Figure 1.1).

1.3.3 PAMPs and DAMPs share the same PRRs

Although DAMPs and MAMPs originate from different sources and are recognized by distinct receptors (Geddes et al., 2009; Mogensen, 2009; Newton and Dixit, 2012; Piccinini and Midwood, 2010), emerging evidence suggests they share many of PRRs, including TLRs and NLRs (Table 1.1).

Table 1.1 Shared TLRs or NLRs between different DAMPs and PAMPs.

Receptor	DAMPs	PAMPs
TLR1	β-defensin-3 (Funderburg et al., 2007)	Triacyl lipopeptides (Takeuchi et al., 2002)
TLR2	β-defensin-3 (Funderburg et al., 2007) HMGB1 (Park et al., 2004, 2006) Antiphospholipid antibodies (Satta et al., 2007) HSP70 (Asea et al., 2002)	Lipoprotein/lipopeptides (Aliprantis et al., 1999) Peptidoglycan/Lipoteichoic acid (Schwandner et al., 1999)

Table 1.1 (Continued).

	Serum amyloid A (Cheng et al., 2008; He et al., 2009) Biglycan (Schaefer et al., 2005)	Atypical lipopolysaccharide (Hirschfeld et al., 2001; Werts et al., 2001) Zymosan (Underhill et al., 1999) Porins (Massari et al., 2002)
TLR4	HMGB1 (Park et al., 2004, 2006) HSP22, 60, 70, 72 (Asea et al., 2002; Ohashi et al., 2000; Roelofs et al., 2006; Wheeler et al., 2009) Biglycan (Schaefer et al., 2005) S100A8, S100A9 (Foell et al., 2007; Vogl et al., 2007) Neutrophil elastase (Devaney et al., 2003) Antiphospholipid antibodies (Mulla et al., 2009) Lactoferrin (Curran et al., 2006) Serum amyloid A (Hiratsuka et al., 2008; Sandri et al., 2008) Saturated fatty acid (Schaeffler et al., 2009; Shi et al., 2006) Biglycan (Schaefer et al., 2005)	Lipopolysaccharide (Chow et al., 1999; Poltorak et al., 1998) Fusion protein (Kurt-Jones et al., 2000) Envelope protein (Rassa et al., 2002) HSP60 (Bulut et al., 2002)

Table 1.1 (Continued).

TLR7/8	Antiphospholipid antibodies (Hurst et al., 2009) ssRNA (Vollmer et al., 2005)	ssRNA (Heil et al., 2004)
TLR9	IgG-chromatin complexes (Leadbetter et al., 2002)	CpG-containing DNA (Hemmi et al., 2000)
NLRP3	ATP (Mariathasan et al., 2006) Uric acid crystals (Martinon et al., 2006) Low potassium concentration (Pétrilli et al., 2007)	Muramyl dipeptide (Martinon et al., 2004) Viral RNA (Kanneganti et al., 2006) Bacterial DNA (Muruve et al., 2008)

1.3.4 Eicosanoid pathways

Eicosanoids are signaling lipid metabolites derived from arachidonic acid or other polyunsaturated fatty acids (PUFAs). Eicosanoids have diverse functions in different pathological processes such as inflammation (Dennis and Norris, 2015).

Phospholipase A_2 (PLA_2) severs as main enzyme which frees arachidonic acid (AA) from its esterified form in phospholipids. There are three members of PLA_2 that contribute the most to AA production including: cytosolic calcium-dependent PLA_2 ($cPLA_2$), cytosolic calcium-independent PLA_2 ($iPLA_2$) and secreted PLA_2 ($sPLA_2$). $iPLA_2$ is mainly involved in maintaining homeostatic cellular functions by producing

low levels of AA constitutively (Dennis and Norris, 2015). However, when homeostasis is disrupted by tissue injury of infection, the increased level of calcium induces the translocation and activation of $cPLA_2$, which leads to elevation of AA and downstream pro-inflammatory eicosanoids (Dennis et al., 2011). As the receptor activation prolongs, $sPLA_2$ is induced and secreted to activate eicosanoids production of the neighboring cells (Fitzpatrick and Soberman, 2001).

AA can be processed into both pro-inflammatory and anti-inflammatory eicosanoids. Cyclooxygenase (COX) and lipoxygenase (LOX) are the two main enzymes that involved in downstream pro-inflammatory signaling pathways. Prostaglandins, the eicosanoids generated from the COX enzyme pathway, are known to induce the key signs of inflammation, such as pain, fever, redness and swelling (Dennis and Norris, 2015). Leukotrienes, the eicosanoids produced in LOX pathway, are documented to serve as early leukocytes chemoattractants after tissue damage (Lämmermann et al., 2013). On the other hand, LOX can also convert AA into anti-inflammatory eicosanoids, such as lipoxins, which can inhibit neutrophil recruitment and increase phagocytosis of apoptotic neutrophils by macrophages at inflammation sites (Lawrence et al., 2002) (Figure 1.2).

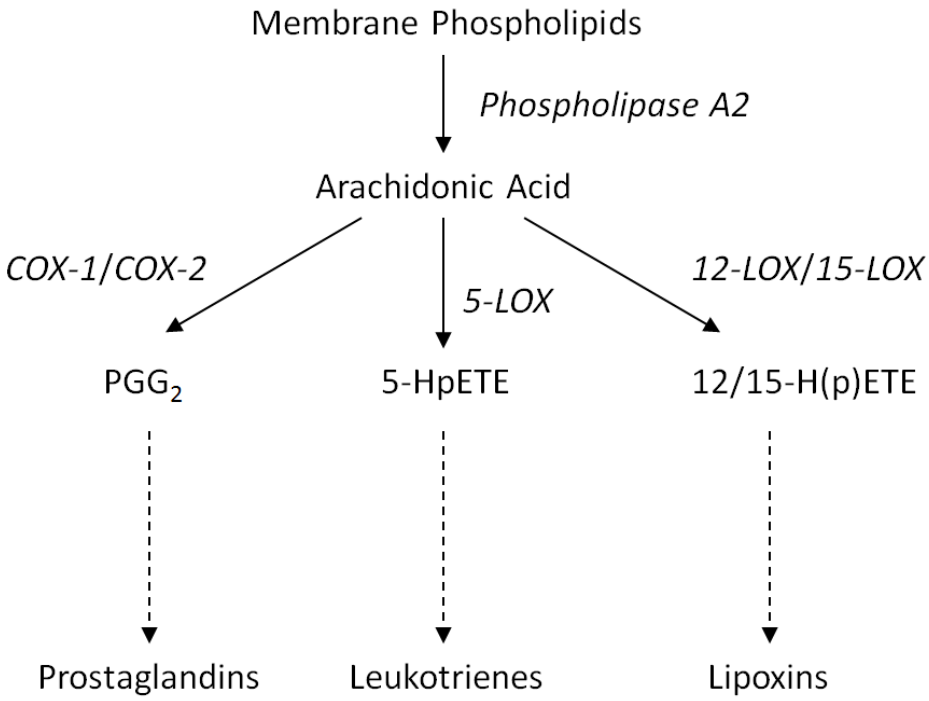

Figure 1.2 Eicosanoid pathways.

1.4 Cell types involved in inflammatory responses

Neutrophils, tissue resident macrophages, mast cells, and epithelial cells are the first cell types that sense the invasion of microbes (Charles A Janeway et al., 2001).

1.4.1 Neutrophils

Neutrophils are the primary defending immune cell types against tissue injury and infection. They constitute the largest portion of the white blood cell population in the circulation (Amulic et al., 2012; Wright et al., 2010).

Patrolling neutrophils constantly probe the endothelial cell surface. Endothelial cells near inflammatory sites express adhesion molecules, such as P- and E-selectins, and integrin members, such as Intercellular Adhesion Molecules (ICAMs), upon stimulation by tissue damage- or microbial-derived inflammatory signals (Borregaard, 2010). As neutrophils move to the inflammatory sites, the glycoprotein P-selectin glycoprotein ligand-1 (PSGL-1) and L-selectins on their surface will interact with P- and E-selectins on endothelial cells (Ley, 2003; McEver and Cummings, 1997). Following the rolling stage, neutrophils further establish a firm adhesion with endothelial cell through neutrophil β2 integrin family proteins interacting with the ICAMs on endothelial cells, which eventually leads to the extravasation of neutrophils to the inflamed tissue (Ley et al., 2007).

After neutrophils enter the interstitial space, tissue-derived cytokines or microbial-derived chemoattractants will bind to their cognate receptors on neutrophils to initiate neutrophil chemotaxis (Amulic et al., 2012). Meanwhile, PRRs on/in neutrophils begin to engage with their ligands and activate downstream proinflammatory pathways as discussed previously.

Upon arrival at inflammatory sites, neutrophils utilize multiple strategies to eliminate pathogens including degranulation, release of antimicrobial peptides/proteins, and generation of reactive oxygen species (ROS) (Mayadas et al., 2014). Neutrophils granules carry a variety of antimicrobial agents including myeloperoxidase (MPO), neutrophil elastase, bactericidal/permeability-increasing protein (BPI), etc.. After

neutrophils are activated, granules translocate and fuse with either plasma membrane or phagosome to release their content to the extracellular space or the phagocytosed pathogens (Lacy, 2006). Additionally, neutrophils can release antimicrobial products, such as α-defensins and lysozyme, directly into the surrounding environment. Furthermore, the production of ROS serves an essential role in antimicrobial action. The nicotinamide adenine dinucleotide phosphate (NADPH) oxidase and MPO are the two main enzymes involved in antimicrobial ROS production in neutrophils. The NADPH oxidase reduces molecular oxygen to superoxide, which is further converted to hydrogen peroxide, hydroxyl radicals and hydroxyl anions. MPO converts hydrogen peroxide into antimicrobial reactive species such as hypochlorous acid (Bogdan et al., 2000).

Following the execution of their antimicrobial function, neutrophils enter resolution phase. The initiation the apoptotic cell-death program serves as the main method for neutrophil clearance (Amulic et al., 2012). Recent studies indicate neutrophils can also undergo reverse migration back to vasculature (Starnes and Huttenlocher, 2012).

1.4.2 Macrophages

Macrophages are white blood cells with multiple functions throughout different stages of inflammation (Mahdavian Delavary et al., 2011).

In the resting stage, macrophages only produce low levels of proinflammatory products (Koh and DiPietro, 2011). Upon exposure to DAMPs, PAMPs or cytokines,

macrophages can enter the “classically activated” (or M1) stage (Mosser, 2003). Those macrophages exhibit proinflammatory functions by secreting large numbers of inflammatory mediators including IL-1, IL-6, TNF-α, and nitric oxide (NO). Meanwhile, macrophages can attract additional leukocytes through the production of chemoattractants such as IL-8 (Arango Duque and Descoteaux, 2014).

On the other hand, macrophage can enter an anti-inflammatory phase upon being “alternatively activated” (or M2) by IL-4 or IL-13 (Gordon, 2003). M2 phase macrophages are capable of secreting anti-inflammatory mediators, such as IL-1 receptor antagonist, as well as growth factors, such as transforming growth factor β (TGF-β) and vascular endothelial growth factor (VEGF). Thus they are critical during the wound healing and angiogenesis process (Gordon, 2003; Koh and DiPietro, 2011).

Another important function of macrophages during the resolution of inflammation is to clear up the wound site. Macrophages carry out such function mainly through phagocytosis of apoptotic debris, which helps to resolve inflammation by preventing secondary necrosis (Koh and DiPietro, 2011).

1.4.3 Leukocytes and sterile inflammation

Although the inflammatory response is essential for protecting the host against invading pathogens, unresolved inflammation or inflammatory responses in the absence infection can lead to various chronic or autoimmune diseases (Chen and Nuñez, 2010). For example, neutrophil infiltration in response to MSU crystals in the

joints can lead to the chronic inflammatory disease gout (Busso and So, 2010). During ischaemia-reperfusion injury, the restoration of blood supply attracts massive amounts of neutrophils. The production of ROS can induce further tissue destruction as seen in myocardial infarction and stroke (Kalogeris et al., 2012). In Alzheimer`s disease, evidence shows that microglial cells adjacent to β-amyloid-containing-plaques can generate ROS as well as other pro-inflammatory cytokines, which cause damage of neurons (Weiner and Frenkel, 2006). Lastly, leukocyte recruitment in the absence of microbial infection is documented to promote tumorigenesis through production of growth factor such as VEGF (Coussens and Werb, 2002).

Section 2: Zebrafish as a model for the study of innate immune responses

2.1 Zebrafish innate immune system

Zebrafish has been extensively used as a model system for hematopoiesis and vertebrate development (Amatruda and Zon, 1999; Bertrand et al., 2007; de Jong and Zon, 2005; Trede et al., 2001). Recently, zebrafish has been appreciated as valuable system to study the immune system and human diseases (Dooley and Zon, 2000; Lieschke and Currie, 2007; Meijer, 2016; Niethammer, 2016; Novoa and Figueras, 2012; Ramakrishnan, 2013a; Renshaw et al., 2007).

Zebrafish has both an innate and an adaptive immune system. While the innate immune system is detectable and functional from day one of zebrafish embryogenesis (Herbomel et al., 1999), its adaptive immune system is not mature until 4 weeks post

fertilization (Trede et al., 2004; Willett et al., 1999). Such temporal separation between innate and adaptive immune system significantly reduces the mechanistic complexity, and allows studying the innate immune system independently from the adaptive immune system.

2.1.1 Cell types in zebrafish innate immune system

Zebrafish immune system comprises almost every immune cell types that found in mammals (Trede et al., 2004). Those cell types include neutrophils, macrophages, eosinophils, and mast cells.

Neutrophils and macrophages are two main cell types involved in zebrafish innate immunity. Upon wounding and/or bacterial infection, neutrophils are the first to migrate and accumulate in damaged tissue (Harvie and Huttenlocher, 2015; Renshaw et al., 2006), macrophages are subsequently recruited to clear up the tissue or bacterial debris (Mathias et al., 2009; Redd et al., 2006).

To date, various leukocyte specific promoters have been identified and used for fluorescent labeling of different cell population, such as the lysozyme C (*lysC*) and the myeloperoxidase promoter for neutrophils (Hall et al., 2007; Renshaw et al., 2006) and the mpeg1 promoter for macrophages (Ellett et al., 2011). These tools enable the real-time, high resolution imaging of neutrophil behavior towards tissue damage or bacterial infection, which is difficult to be achieved in other vertebrate model systems such as mice.

Zebrafish has been used to understand the very first signals that are involved in inflammatory response. One mechanism is nuclear swelling which acts as a mechanical activation signal for inflammatory lipid signaling to attract neutrophils to sites of tissue damage (Enyedi et al., 2013, 2016). Namely, fish interstitium is exposed through tailfin wounds to bathing media with lower osmolarity. Hypotonic exposure-induced nuclear membrane stretch promotes the translocation and activation of $cPla_2$, which cleaves phospholipids in to proinflammatory lipid precursors such as arachidonic acid (Figure 1.3). *In vivo* imaging of fluorescently labeled neutrophils greatly facilitated these studies. These studies highlight the progress that has been made for the important role of nonlytic stress signals during the fast tissue damage detection (Enyedi and Niethammer, 2017; Enyedi et al., 2013, 2016).

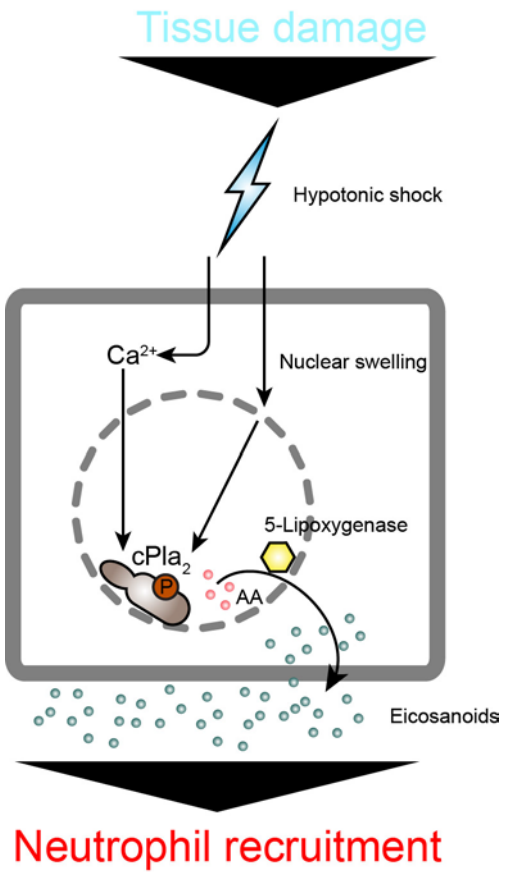

Figure 1.3 Schematic view of tissue damage induced $cPla_2$ activation.

Zebrafish also provides a unique platform for studying the contribution of macrophages to infectious disease in the context of a whole living organism (Masud et al., 2017; Torraca et al., 2014). For example, researchers have successfully established a TB disease model by infecting zebrafish with *Mycobacterium marinum*, a close genetic relative to the human TB pathogen, *Mycobacterium tuberculosis* (Meijer, 2016; Ramakrishnan, 2013b). Zebrafish overcome the limitation of mouse models, which lack the compact necrotic granulomas (Flynn, 2006), as well as the risk of working with the airborne transmitted human pathogen. By using the zebrafish TB model, researchers have demonstrated that macrophages suffice for initiation of

granulomas independent of adaptive immunity (Davis et al., 2002). Moreover, this model also shows that granulomas promote the expansion and dissemination of infection, which changes the historically widespread view of a host-protective role of granulomas (Davis and Ramakrishnan, 2009; Ramakrishnan, 2012).

2.1.2 Immune proteins and genes in zebrafish innate immune system

Many innate immune mediators and genes are conserved between zebrafish and mammals (Stein et al., 2007). Zebrafish possesses multiple human TLR homologues(TLR1/2/3/4/5/7/8/9) as well as several zebrafish specific TLRs(TLR18/19/20/21/22) (van der Vaart et al., 2012). Not all the ligands for fish TLRs are identified. Previous studies have shown the conservation of ligand recognition by some TLRs between fish and humans (e.g. lipopeptides for TLR2, dsRNA for TLR3 and flagellin for TLR5) (Matsuo et al., 2008; Ribeiro et al., 2010; Stockhammer et al., 2009). Additionally, dsRNA and Poly:C have been identified as the ligand of TLR22 (Matsuo et al., 2008). However, zebrafish TLR4 has different extracellular domains comparing to mammals. As a result, fish TLR4 is not able to respond to LPS (Sepulcre et al., 2009; Sullivan et al., 2009). Besides the TLRs, key adaptor proteins of the TLR signaling pathway also exist in zebrafish, including MyD88, TIRAP, TRIF, TRAF6, and IRF3/7 (Novoa and Figueras, 2012; Purcell et al., 2006). MyD88 and TRAF6 are required for bacteria induced inflammatory responses (van der Sar et al., 2006; Stockhammer et al., 2010). Moreover, the fish TLR signaling triggers similar transcriptional factor families including NF-κB, AP-1, ATF (activating transcription factor), IRF, and STAT (signal transducer and activator of

transcription) (Ordas et al., 2011; Stockhammer et al., 2009; van der Vaart et al., 2012).

Three subfamilies of NLRs have been identified in zebrafish. The first subfamily contains the orthologues of mammalian NODs, which includes NOD1, NOD2, NLRC3, CIITA (the Major Histocompatibility Class (MHC) II transactivator), Apaf1 (apoptotic protease activating factor 1) and NLRC5. The second subfamily resembles the mammalian NALPs including NLRP6, NLRB5 and NLRC3-like. The third subfamily is a fish specific group of NLR proteins, which contains several hundreds of members (Howe et al., 2016; Laing et al., 2008; van der Vaart et al., 2012). Knockdown of zebrafish NOD1 and NOD2 decreases dual oxidase (DUOX) expression and larval survival upon bacterial infection, which suggests their involvement in antibacterial function (Oehlers et al., 2011). Moreover, zebrafish NLRC5 is involved in antiviral immune responses and transcriptional regulation of MHC class II genes (Wu et al., 2017). These studies illustrate the conserved role of NLRs in antibacterial and antiviral functions.

2.1.3 Immune effectors in the zebrafish innate immune system

Cytokines, including chemokines, interleukins, and interferons, are largely conserved between zebrafish and mammals (Stein et al., 2007). Several interleukin members, including IL1β, IL6, and IL10, have been characterized in zebrafish (Huising et al., 2004; Varela et al., 2012; Zhang et al., 2005). However, zebrafish IL1β lacks the

traditional mammalian caspase-1 cleavage site while containing multiple alternative cleavage sites (Angosto et al., 2012; Vojtech et al., 2012). Nevertheless, fish IL1β maintains its function in promoting inflammatory response during *Pseudomonas aeruginosa* infection (Clatworthy et al., 2009) and tissue regeneration (Kyritsis et al., 2012).

A previous study has shown that fish TNF signaling protects a host from mycobacteria infection, where macrophage death and granuloma formation increase after the knockdown of TNF receptor (Clay et al., 2008). Additionally, fish TNF-α has been shown as an activator of chemokine production in endothelial cells, where it mainly functions to recruit leukocytes (Roca et al., 2008).

As in humans, zebrafish have three groups of interferons. The group I INFs induce antiviral gene expression against myxovirus infection (Altmann et al., 2003). Zebrafish possesses two group II INF genes, namely IFN-γ1 and IFN-γ2 (Aggad et al., 2010). While the proinflammatory and antigen presentation functions are conserved (López-Muñoz et al., 2011), they fail to protect zebrafish from bacterial and viral infection (López-Muñoz et al., 2009).

Oxidative defense is conserved in zebrafish. Actually, using zebrafish, it has been shown for the first time that hydrogen peroxide (H_2O_2), generated by oxidase activity of DUOX, functions as a mediator for rapid wound detection (Niethammer et al., 2009). However, it was proposed that H_2O_2 is not generated during bacterial infection

(Deng et al., 2012). Subsequently, Lyn, a Src family kinase member, was identified as H_2O_2 sensor in neutrophils mediating the attraction of leukocyte to the wound (Yoo et al., 2011). Moreover, the antibacterial function of DUOX in zebrafish innate immunity protects fish during intestinal infection (Flores et al., 2010).

Taking together, the major components involved in zebrafish innate immune response are highly conserved between fish and mammals.

2.2 Additional advantages of zebrafish model

Zebrafish has been established as genetic tractable model system since the 1980s (Streisinger et al., 1981). Compared to mice, they are cheaper to maintain. The mating of zebrafish is triggered by the break of daylight (Hisaoka and Firlit, 1962). Each pair of adult zebrafish can produce large number of offspring, usually hundreds of embryos per week (Patton and Zon, 2001). Zebrafish develop fast. Most organs are present at 24 hour post fertilization. Fish can reach sexual maturity at 3 months (Kimmel et al., 1995).

Zebrafish larvae are nearly transparent. A transgenic line of pigmentation mutation has also made zebrafish transparent throughout its life time (White et al., 2008). These features make zebrafish particularly suited as intravital imaging model for studying inflammatory response and cancer progression (Enyedi et al., 2013; Feng and Martin, 2015; Heilmann et al., 2015; Ignatius et al., 2016; Niethammer et al., 2009; Renshaw et al., 2007; Tulotta et al., 2016).

The zebrafish genome is largely conserved comparing to human. Approximately 70% of genes are shared between those two species. 84% of human disease related genes have counterparts in zebrafish (Howe et al., 2013). Various tools have been developed for the genome editing in zebrafish including morpholino knockdown and CRIPSR/Cas9 (Hruscha et al., 2013; Jao et al., 2013; Nasevicius and Ekker, 2000).

To date, large scale genetic as well as drug screens have been conducted using zebrafish because of its advantages mentioned above (Driever et al., 1996; Haffter et al., 1996; Robertson et al., 2014; Takaki et al., 2012; Wittmann et al., 2015).

Lastly, zebrafish serve as a powerful model for studying human mucosal skins. Although human dry epidermis covers an area about 2 m^2 (Hadgraft, 2001), it only accounts for ~ 1-10 % of total surface area of an adult human (Helander and Fändriks, 2014; Niess and Reinecker, 2006), depending on the specific measuring method. Thus, most of the human surface area is covered by mucosal lining. Especially, the human upper digestive track is covered by saliva, a hypotonic solution. Thus, zebrafish serves as a great model for studying the mucosal injury of human.

Chapter II: Experimental Results

Section 1: Introduction

Tissue damage or infection can trigger inflammatory responses by the innate immune system, including the fast infiltration of neutrophils to the damaged or infected tissue. While the recruitment of neutrophils is generally beneficial against bacterial infection, the physiological purpose of tissue damage induced ("sterile") neutrophil infiltration is largely unknown. Upon the release of toxic enzymes, neutrophils can cause additional damage to the host and thus delay the healing and regeneration process of injured tissue (Dovi et al., 2003, 2004; Schofield et al., 2013; Simpson and Ross, 1972). Do these deleterious functions of neutrophils reflect a "design flaw" of innate immune system? Or do they provide some selective advantages to the host? To address this question, we set out to test the potential contributions of tissue damage signals to antimicrobial immune responses.

Although this idea seems intuitive, no previous research, to our knowledge, has ever been conducted to test it. This is largely due to the difficulty of selectively blocking the tissue damage induced signaling in the context of bacterial infection. After all, all current methods, such as injection, that deliver bacteria into the host will inevitably cause host tissue damage. Besides, bacterial and tissue damage induced signals share a common set of PRRs, which precludes the selective downstream inhibition of tissue damage.

To date, many research groups have shown that sterile inflammatory signals are sufficient to trigger neutrophil recruitment *in vivo* (Lämmermann et al., 2013; McDonald et al., 2010; Ng et al., 2011). Previous *in vitro* studies also indicate some PAMPs as potent neutrophils chemoattractants (Bloes et al., 2015). As microbial cues act through similar pattern recognition pathways, PAMPs are thought to suffice for local neutrophil responses as well. However, this fundamental assumption has never been thoroughly tested before. Additionally, since it is difficult to elucidate and eliminate every DAMP, it is very challenging to test the contribution of tissue damage signaling to microbial detection in the canonical way (Kono and Rock, 2008).

To this end, zebrafish serve as an alternative model organism which enables more feasible experimental design. Zebrafish innate immune system is highly conserved as compared to mammals (Trede et al., 2004). At 2-3 days post fertilization, zebrafish innate immunity is fully developed while the adaptive immune system is still absent (Trede et al., 2004), which provides a unique temporal gap to investigate the mechanism of innate inflammatory responses. Furthermore, the transparency feature of zebrafish larvae facilitates intravital live imaging. Upon wounding, the exposure of zebrafish interstitial tissue to environmental fresh water induces cell swelling around the wound due to the difference of osmotic pressure. Although cell swelling is a common pathological hallmark of tissue damage in all animals (Liang et al., 2007; Majno and Joris, 1995; Vanden Berghe et al., 2014), its direct inflammatory function has only been studied in zebrafish so far. In zebrafish, cell and nuclear swelling serve

as a mechanical transducer that triggers the translocation and activation of $cPla_2$, which cleaves arachidonic acid from phospholipids, a prerequisite for the synthesis of proinflammatory eicosanoids (Enyedi et al., 2013, 2016; Niethammer et al., 2009). Cell swelling is abrogated by bathing larvae in isotonic solution, which provides a unique way to shut down tissue damage induced inflammatory signaling in the context of infection.

Section 2: Results

2.1 Microbial ear infection triggers heterogeneous neutrophil responses in zebrafish larvae

To generate focal infection in zebrafish, *Pseudomonas aeruginosa* (PA) or *Escherichia coli* (*E. coli*) resuspended in either hypotonic or isotonic E3 medium was injected into the otic vesicle (inner ear) of three day old larvae (Figure 2.1A) as previously described (Deng et al., 2012). The suspensions were supplemented with 1 μm fluorescent beads to label the infection site. The beads acted as bright and faithful fluorescent proxy for bacterial dispersion, similar to fluorescent PA (Figure 2.1B, C). Assuming a spherical shape, we estimated the ear volume to ~1 nL. To rupture the luminal ear integument by overpressure, we injected a ~ two times larger volume (2.3 nL) of PA suspension. The damage induced by the injection (Figure 2.1D) gives microbes and bathing solution access to the fish interstitium and allows rapid equilibration of ear fluid and bathing solution, as indicated by the quick loss of 4 kD dextran fluorescence from the ear lumen (Figure 2.1E).

A neutrophil-specific reporter *lysC* (Hall et al., 2007) was used to fluorescently label the neutrophil population in the fish line. Injected fish larvae were imaged for 90 minutes by time-lapse microscopy. Under standard, hypotonic bathing condition (Hypo+PA), infection triggered strong leukocyte recruitment in ~ one third of the animals (Figure 2.1C, "High Responders", HR). These strong responses were characterized by the synchronized convergence of neutrophils onto the ear infection site. Two thirds of the animals displayed sporadic, unsynchronized neutrophil migration (Figure 2.1C, "Low Responders"). The relative high number of observed animals facilitated appreciation and quantification of this response heterogeneity. Although the precise factors that contribute to it remain unclear, we speculate that biological thresholds, (epi-)genetic variability, and stochasticity of injection-induced ear rupture, might play a role. To unbiasedly classify the phenotype (Figure 2.1C), blinded neutrophil recruitment curves were randomly selected from a pool of ~1600 experiments across 41 experimental conditions, and manually grouped into high and low responder "training sets". The threshold was automatically calculated from those training sets and used for subsequent classification of the remaining neutrophil curves. The HR-index (HR_i) represents the frequency of high responders in each experimental group. To ensure the robustness of our method, unsupervised Gaussian mixture distribution model without user-defined training sets was used to automatically cluster the same data set, and yielded similar results (Figure 2.1C).

Figure 2.1 Ear infection of zebrafish larvae with *Pseudomonas aeruginosa* (PA) triggers strong neutrophil responses in a subset of animals.

(A) Cartoon scheme of experiment. (B) Ear injection of microbes generates a localized source of infection as visualized with EGFP-tagged PA (shown: hypotonic bathing conditions). (C) Upper panel, representative time-lapse montage of neutrophil recruitment to infected ears in a Low Responder (left) versus a High Responder (right) animal at indicated times. Neutrophils are in red. Cyan fluorescent beads mark the ear region. Scale bar, 100 μm. Lower panel, neutrophil recruitment kinetics in Hypo+PA fish computationally classified into low (black) and high (red) responders by comparison to user-generated training sets. High responder index is depicted as pie chart. Blue percentage, an unsupervised (that is, no user-defined training sets) Gaussian distribution clustering algorithm determines a similar HR-index. (D) Representative image of injection-induced ear damage under hypotonic (left) and isotonic (right) bathing conditions. The nuclei of damaged cells are stained with the cell lysis dye SYTOX orange. Scale bar, 100 μm. (E) Fluorescence of 4 kD dextran is quickly lost (Right) comparing to cyan fluorescent beads (Left) that are injected at the same time. Upper panel: 0 min; lower panel: 90 min. Scale bar, 100 μm.

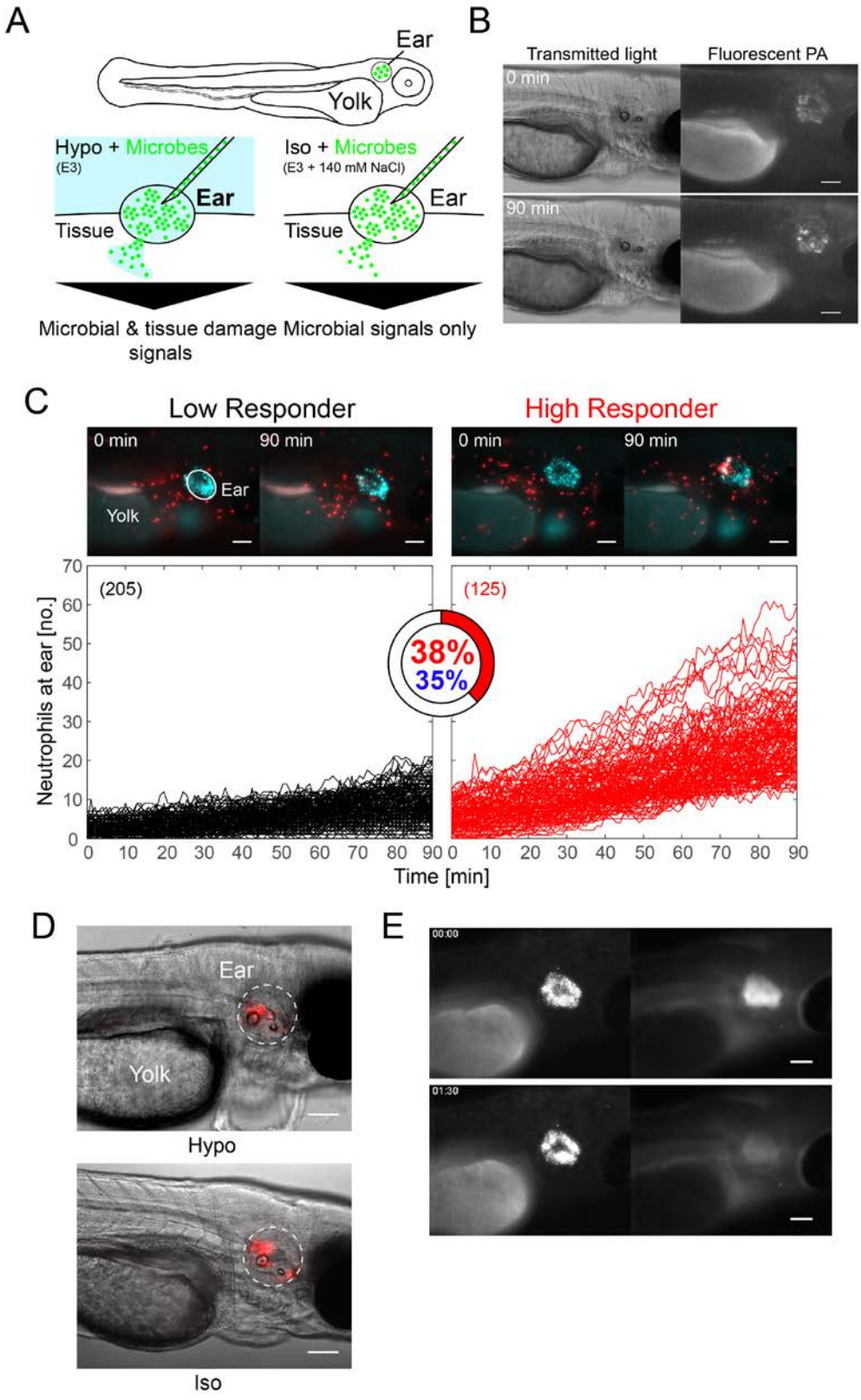
A
Ear
Yolk
Hypo + Microbes
(E3)
Ear
Tissue
Iso + Microbes
(E3 + 140 mM NaCl)
Ear
Tissue
Microbial & tissue damage signals
Microbial signals only
B
Transmitted light
Fluorescent PA
0 min
90 min
C
Low Responder
High Responder
0 min
90 min
Ear
Yolk
(205)
(125)
38%
35%
Neutrophils at ear [no.]
Time [min]
D
Ear
Yolk
Hypo
Iso
E
00:00
01:30

2.2 Selective suppression of tissue damage signals inhibits protective neutrophil recruitment to infections

In cell culture experiments, microbes suffice for attracting neutrophils through formylated peptides, and other emitted chemotactic factors (Nuzzi et al., 2007; Schiffmann et al., 1975). Serum is often present before or during these experiments, possibly mimicking aspects of a wound microenvironment. Likewise, the isolation of primary neutrophils involves injury-inducing procedures. Although these *in vitro* assays are valuable for dissecting fundamental chemotactic signaling mechanisms, it is uncertain which—if any—physiological state they resemble.

Ear infection of PA under isotonic condition (Iso+PA) largely abolished neutrophil recruitment, even though the increase of osmolarity did not alter the viability of the bacteria (Figure 2.2A). Additionally, SYTOX orange staining of injected ear indicated comparable level of cell lysis under hypotonic and isotonic condition (Figure 2.1D), which is in line with our previous tailfin wounding assay (Enyedi et al., 2013; Gault et al., 2014). Although high responders, undistinguishable from those under hypotonic conditions, were still present in the absence of tissue damage cues during PA infection, their frequency dropped dramatically (Figure 2.2B). The high responder group was totally abrogated when infecting fish with non-pathogenic *E. coli* (TOP10) (Figure 2.2B, C). The basal level of high responders observed in PA but not *E. coli* infection led us to investigate potential role of PA cytotoxicity in recruiting neutrophils (Dacheux et al., 2001). As mentioned above, necrotic cell demise involves cell- and organelle swelling even under isotonic conditions. PA

phospholipase ExoU, a major virulent effector of type III secretion system, disrupts the plasma membrane to induce cell necrosis (Finck-Barbançon et al., 1997; Hauser and Engel, 1999). Indeed, infecting fish with ExoU mutant PA strain (PA *exoU*) further decreased neutrophil recruitment compared to the wt PA strain under isotonic condition (Figure 2.2B, D). Remaining neutrophil responses may be due to residual, ExoU-independent cytotoxicity. Importantly, co-injecting PA *exoU* together with the non-microbial membrane disruptors melittin (naturally occurs in venom of *Apis mellifera*, honeybee) and digitonin (naturally occurs in *Digitalis purpurea*, foxglove), respectively, restored neutrophil recruitment (Figure 2.2B, D). Melittin, but not digitonin, moderately decreased bacterial viability, in line with melittin's known antimicrobial functions (Picoli et al., 2017) (Figure 2.2E), but control experiment with heat-killed PA excluded the effect of bacteria viability on neutrophil recruitment (Figure 2.2F, G). Altogether, these experiments argue that necrosis, for instance, induced by bacterial virulence, can functionally replace extracellular hypotonicity to some extent. This makes a broad case for tissue damage signaling—osmotic or otherwise—as essential trigger of antimicrobial neutrophil responses *in vivo*.

Figure 2.2 Selective suppression of tissue damage signaling abrogates neutrophil responses to infection sites.

(A) Average bacterial viability analysis as a function of extracellular tonicity. Error bars, SEM of n different agarose plates. (B) HR indices after PA or *E. coli* infection in the presence (Hypo) or absence (Iso) of osmotic tissue damage signaling, and as a function of microbial cytotoxicity (ExoU). HR indices are depicted as pie charts. Asterisks, Fisher's exact test $p<0.05$. Note, the Hypo + PA reference set is the same as in the other figures. Parentheses, number of injection experiments. (C) Average neutrophil recruitment to *E. coli* infected ears in zebrafish larvae in the presence (Hypo + *E. coli*, black) or absence (Iso + *E. coli*, red) of tissue damage signals. Shaded area, SEM of n injection experiments. (D) Average neutrophil recruitment as a function of endogenous, microbial (ExoU) and exogenous (digitonin, melittin) cytotoxicity. Shaded area, SEM of n injection experiments (parentheses). (E) Bacterial viability analysis in response to digitonin or melittin treatment. Error bars, SEM of n different agarose plates. Asterisk, t-test $p<0.05$. (F) Average neutrophil recruitment to live (grey) or heat-killed (hk, red) PA. Shaded area, SEM of n aggregated animal experiments. Note, reference data set (Hypo + PA) is the same as in the other figures. (G) Bacterial viability analysis as a function of heat-killing. Error bars, SEM of n different agarose plates.

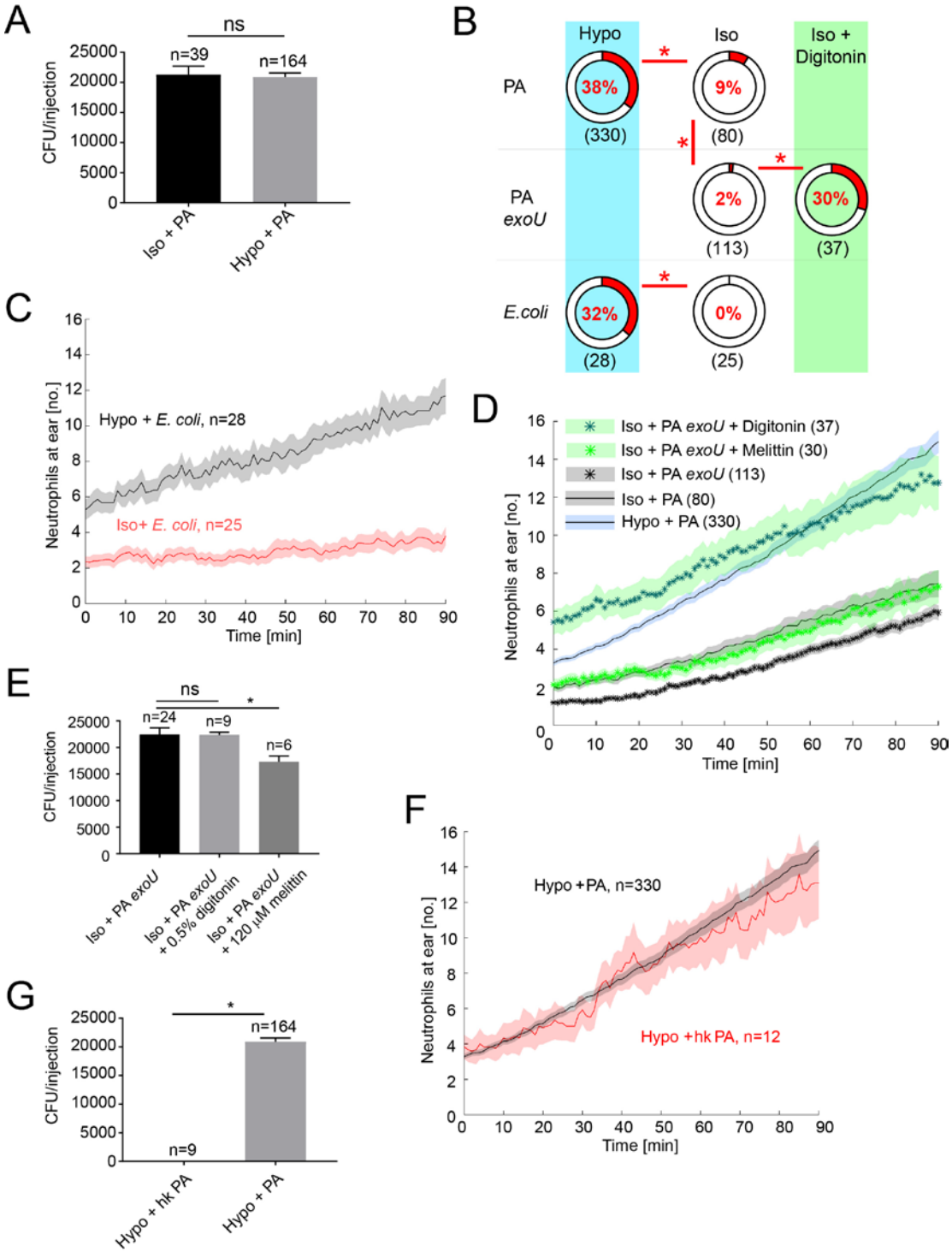
A
ns
n=39
n=164
CFU/injection
25000
20000
15000
10000
5000
0
Iso + PA
Hypo + PA
B
Hypo
Iso
Iso + Digitonin
PA
38%
(330)
9%
(80)
PA exoU
2%
(113)
30%
(37)
E.coli
32%
(28)
0%
(25)
C
Neutrophils at ear [no.]
Hypo + E. coli, n=28
Iso+ E. coli, n=25
Time [min]
D
Iso + PA exoU + Digitonin (37)
Iso + PA exoU + Melittin (30)
Iso + PA exoU (113)
Iso + PA (80)
Hypo + PA (330)
Neutrophils at ear [no.]
Time [min]
E
ns
*
n=24
n=9
n=6
CFU/injection
Iso + PA exoU
Iso + PA exoU + 0.5% digitonin
Iso + PA exoU + 120 µM melittin
F
Hypo +PA, n=330
Hypo +hk PA, n=12
Neutrophils at ear [no.]
Time [min]
G
*
n=164
n=9
CFU/injection
Hypo + hk PA
Hypo + PA

Neutrophil migration parameters (speed, trajectory length, and persistence) were significantly reduced under isotonic as compared to hypotonic infection conditions (Figure 2.3A). However, random neutrophil movement was not affected by isotonicity in uninjected fish larvae (Figure 2.3A). Together with the observation of residual high responder under isotonic infection (Figure 2.2B) and our previous finding of externally added eicosanoids could rescue isotonic inhibition of neutrophil migration (Enyedi et al., 2013), a generalized inhibition of neutrophil motility by bath tonicity is precluded. Moreover, bacterial viability was not affected by isotonic treatment in all experimental groups (Figure 2.3B). Thus, epithelium damage is required for osmotic regulation of neutrophil responses. To confirm our observation was not correlated to a specific tissue, e.g. inner ear, we performed the PA infection experiment in fish trunk muscle, and observed similar results as ear infection assay (Figure 2.3C, D).

Figure 2.3 Selective suppression of tissue damage signaling inhibits neutrophil movement to infection sites, and decreases the survival of infected zebrafish larvae.

(A) Neutrophil tracking analysis. Top panel, images representative of n (parentheses) injection experiments. Lower panel, table of leukocyte migration parameters. v, migration velocity. l, path length. D_p, directional persistence. Shown are average values ± SEM for indicated number of injection experiments (parentheses). Asterisks, one-way Anova between indicated groups $p<0.05$. Scale bar, 100 μm. (B) Meier-Kaplan plots of post-infection survival of PA-infected larvae in the presence or absence of osmotic tissue damage signaling. Different lines in each graph refer to different PA concentrations. Asterisks, log-rank test $p<0.05$. Parentheses, number of injection experiments. (C) Top, scheme of alternative injection site. Bottom, representative still images of neutrophil recruitment to muscle infection sites at indicated times in the presence (Hypo) and absence (Iso) of tissue damage signals. Arrow, injection site. Scale bar, 100 μm. (D) Average neutrophil recruitment to muscle injection sites as a function of osmotic tissue damage signaling. Shaded area, SEM of n injection experiments (parentheses).

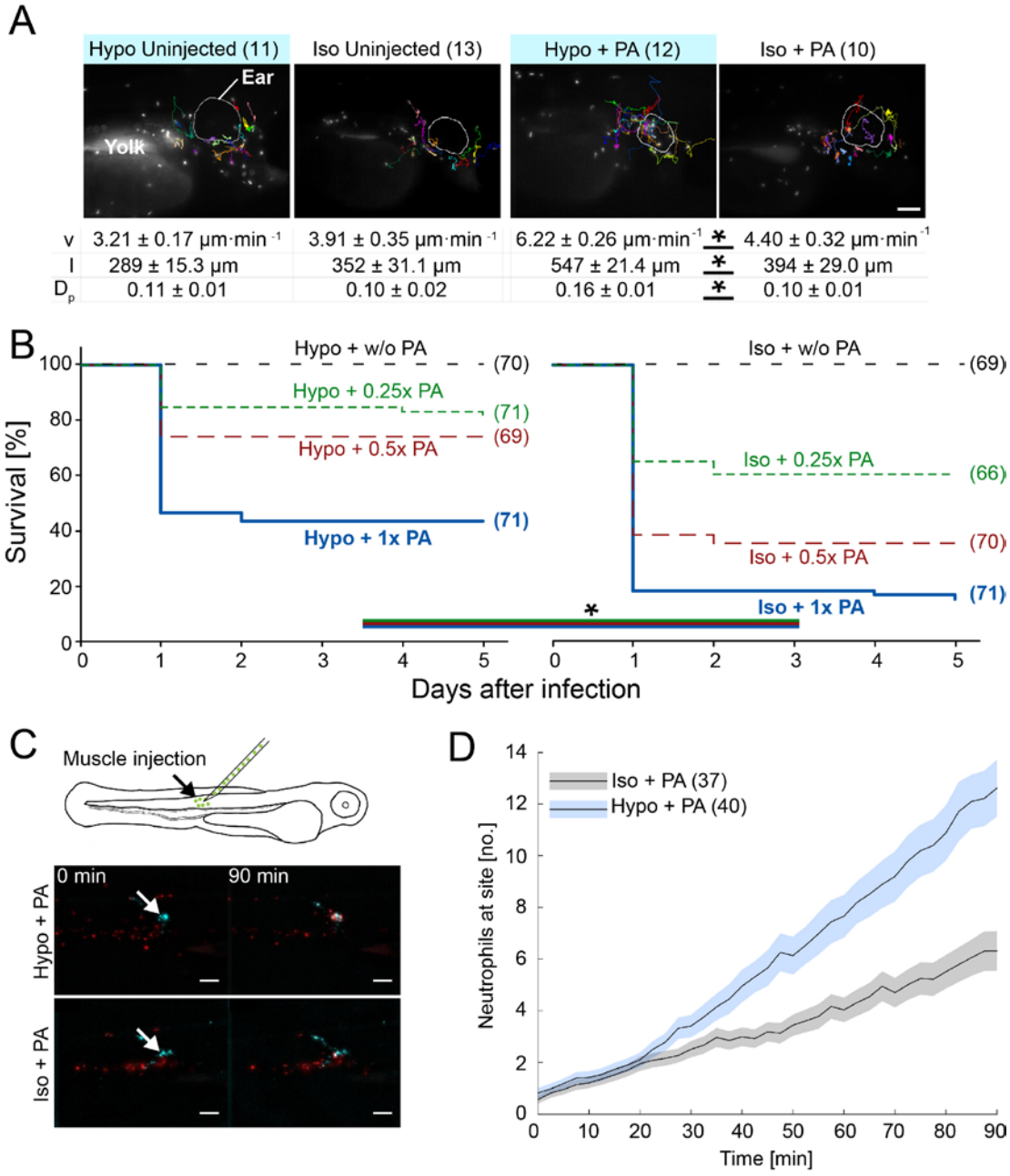
A
Hypo Uninjected (11)
Iso Uninjected (13)
Hypo + PA (12)
Iso + PA (10)
Ear
Yolk
v 3.21 ± 0.17 µm·min -1 3.91 ± 0.35 µm·min -1 6.22 ± 0.26 µm·min -1 * 4.40 ± 0.32 µm·min -1
l 289 ± 15.3 µm 352 ± 31.1 µm 547 ± 21.4 µm * 394 ± 29.0 µm
Dp 0.11 ± 0.01 0.10 ± 0.02 0.16 ± 0.01 * 0.10 ± 0.01
B
Hypo + w/o PA (70)
Hypo + 0.25x PA (71)
Hypo + 0.5x PA (69)
Hypo + 1x PA (71)
Iso + w/o PA (69)
Iso + 0.25x PA (66)
Iso + 0.5x PA (70)
Iso + 1x PA (71)
Survival [%]
Days after infection
C
Muscle injection
0 min
90 min
Hypo + PA
Iso + PA
D
Iso + PA (37)
Hypo + PA (40)
Neutrophils at site [no.]
Time [min]

Transcriptional induction of chemokines is a well-known signaling event for canonical innate immune responses against PAMPs and DAMPs. We wondered whether hypotonicity may stimulate rapid neutrophil recruitment through regulating chemokine expression. However, bathing fish with cycloheximide (CHX), a protein synthesis inhibitor, had little effect on neutrophil recruitment (Figure 2.4A, B), which argued against the involvement of transcriptional gene regulation during early neutrophil responses.

Figure 2.4 Effects of pharmacological treatments on neutrophil recruitment to the infected ear of zebrafish larvae.

(A) Summary of pharmacologic pathway perturbations (indicated below graph). All compounds were applied by ear injection and bathing. The tonicity of the injection solution is always the same as the bath tonicity. Two measurements are given: the HR-index (red, pie charts), and average leukocyte recruitment curves (orange, 3-timepoint-plot format: 0', 45', 90', see Figure 4.1). The color shading indicates combinatorial experimental conditions as indicated on the right side. Error bars, SEM. Parentheses, number of animals per condition. Orange lines, t-test $p<0.05$ (comparison of average leukocyte numbers at 90'). DMSO ctr, carrier control. CHX, cycloheximide. (B) Phenotype classification by user-unsupervised (i.e., without manually selected training sets) Gaussian mixture distribution model clustering. Blue numbers, HR index. Middle panel shadings indicate combinatorial experimental conditions as indicated on the right side. Note, data sets are the same as in other figures.

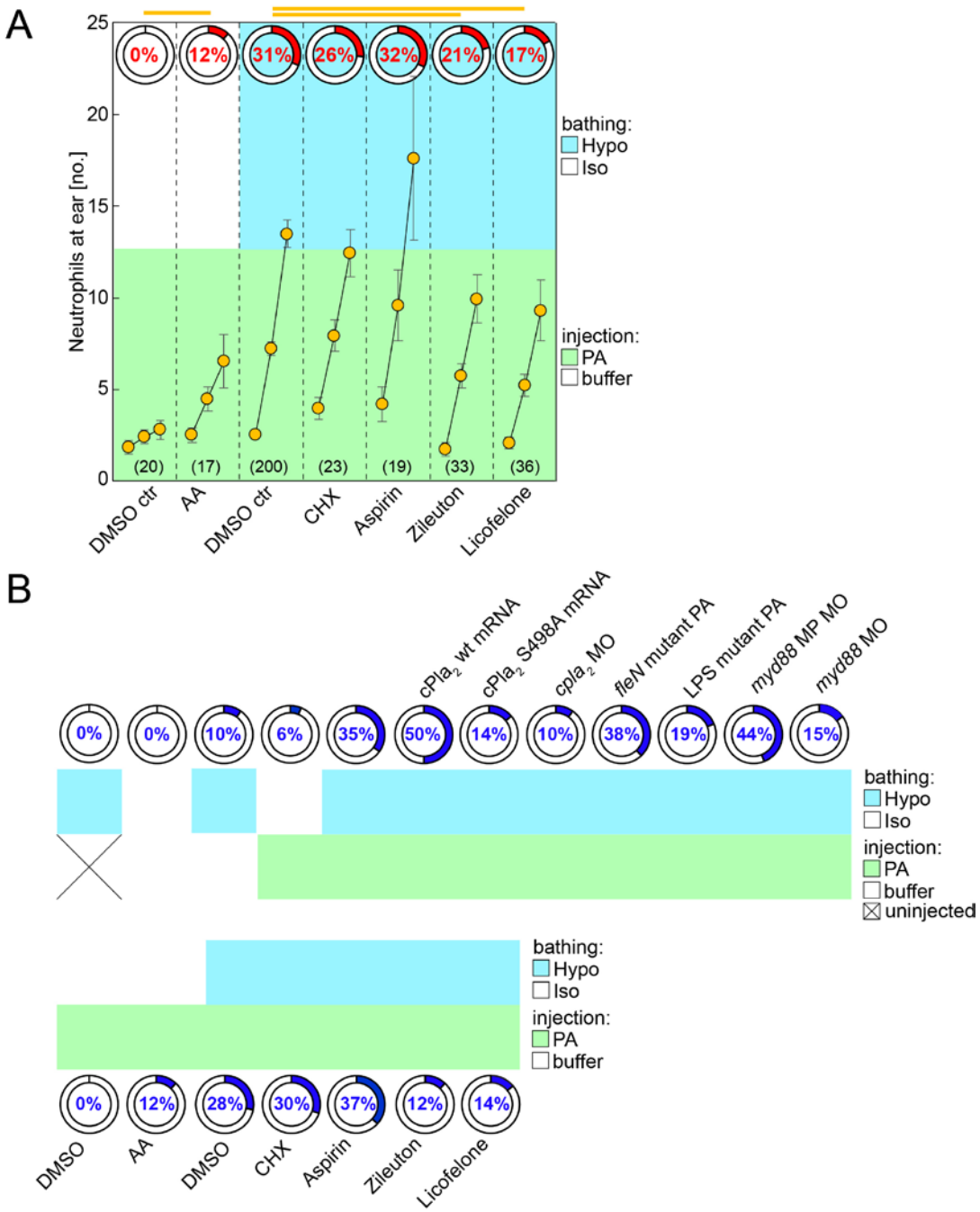
A
Neutrophils at ear [no.]
0%
12%
31%
26%
32%
21%
17%
bathing:
Hypo
Iso
injection:
PA
buffer
(20)
(17)
(200)
(23)
(19)
(33)
(36)
DMSO ctr
AA
DMSO ctr
CHX
Aspirin
Zileuton
Licofelone
B
cPla2 wt mRNA
cPla2 S498A mRNA
cpla2 MO
fleN mutant PA
LPS mutant PA
myd88 MP MO
myd88 MO
0%
0%
10%
6%
35%
50%
14%
10%
38%
19%
44%
15%
bathing:
Hypo
Iso
injection:
PA
buffer
uninjected
bathing:
Hypo
Iso
injection:
PA
buffer
0%
12%
28%
30%
37%
12%
14%
DMSO
AA
DMSO
CHX
Aspirin
Zileuton
Licofelone

The HR-index turned out to be predictive of post-infection survival. In the presence of tissue damage signals, 38% of the larvae exhibited strong neutrophil responses, with 44% surviving. Without tissue damage signals, only 9% of the animals showed strong neutrophil recruitment, and only 15% survived (Figure 2.2B, 2.3B). Notably, infected fish larvae were only kept in isotonic bathing solution for the first two hours after infection. Thus immediate damage signaling is crucial for fish survival after bacterial infection, providing a selective advantage.

2.3 Suppression of osmotic damage does not abrogate microbe recognition

To investigate transcriptional responses to ear infection under different osmotic conditions, mRNA sequencing was performed to three groups of fish: uninfected larvae, larvae infected with PA in hypotonic (Hypo+PA) and isotonic (Iso+PA) bathing solution. Comparing uninfected larvae with larvae infected with PA in hypotonic (Hypo + PA), or isotonic (Iso + PA) bathing solution showed that tissue damage signaling was required for full, transcriptional responses to PA-infection (that is, two times up- or down-regulation of 100 genes; Figure 2.5A, Table 5.1 and 5.2), which indicated tissue damage signaling was indispensible for activating full transcriptional responses. Nevertheless, microbial signals alone induced a subset of immune genes including AP-1 subunits (*fosl1*, *junba*, *junbb*), cyclooxygenase 2 (*ptgs2b*), Il1β (*il1b*) and NADPH oxidase organizer 1a (*noxo1a*), which are known to be induced by bacterial LPS (Eliopoulos et al., 2002; Forn-Cuní et al., 2017; Kawahara et al., 2005; van der Vaart et al., 2013) (Figure 2.5A). Even without microbial cues, tissue wounding is known to induce expression of AP-1 subunits, IL-

1β, and PTGS2 genes (Chen and Nuñez, 2010; Fitsialos et al., 2007). This may explain why the absence of hypotonic wound cues blunted their induction. Additionally, whole mount *in situ* hybridization showed strong and systemic *il1b* mRNA expression in both hypotonic and isotonic conditions (Figure 2.5B). Taking together, fish larvae were able to recognize microbial cues and induce robust upregulation of important inflammatory genes even without osmotic tissue damage signaling.

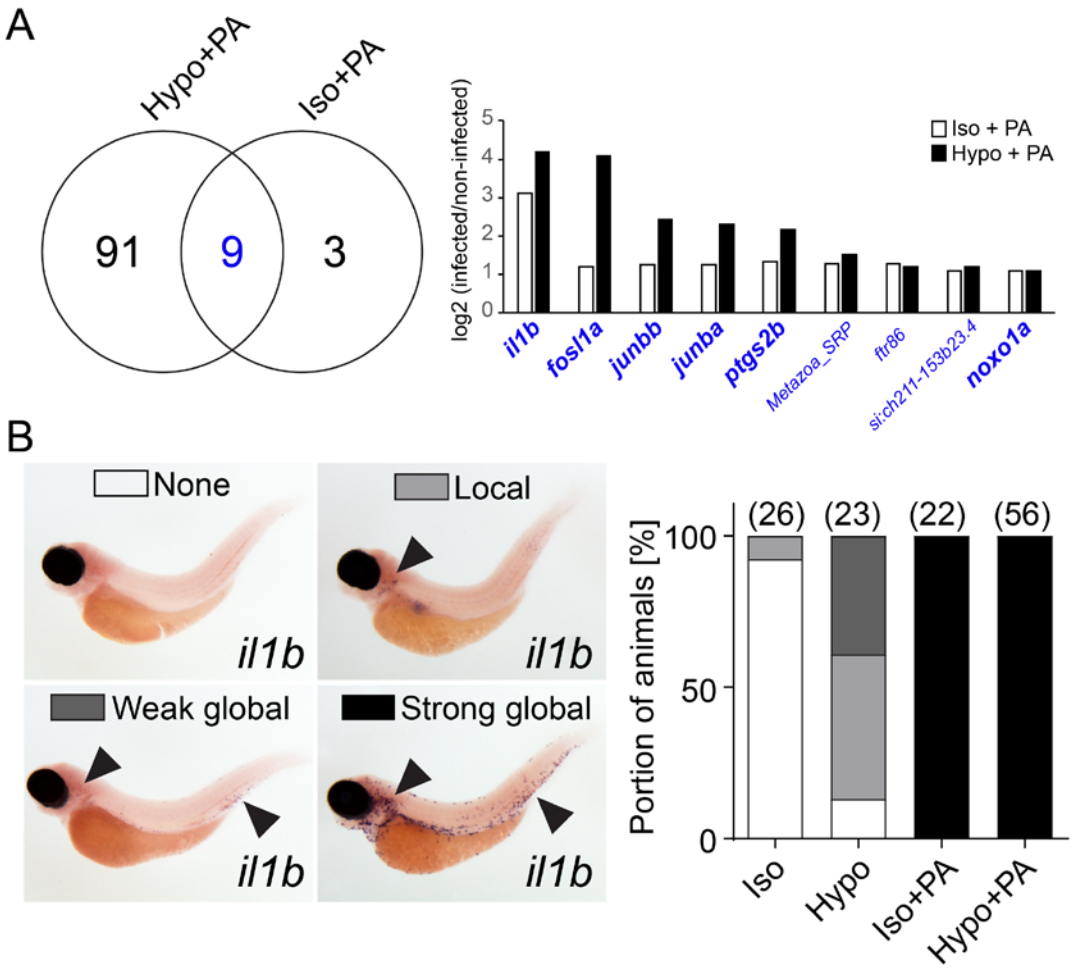

Figure 2.5 Absence of tissue damage signaling does not block microbial detection.

(A) Left panel, Venn plot of significantly (p_{adj}<0.05), at least two times up- or down-regulated mRNAs at 60 min after PA ear infection in the absence (Iso+PA) or presence (Hypo+PA) tissue damage signaling. Right panel, log2-fold regulation of intersection gene set (blue). Bold italics, known LPS-downstream effectors. See Table 5.1 and 5.2 for more detail. Results are derived from n=3 independent mRNAseq experiments. (B) *In situ* hybridization for *il1b* mRNA. Left panel, representative images of different classes of staining patterns observed in indicated number of injection experiments (parentheses, right panel). Right, quantification of staining pattern frequency.

2.4 $cPla_2$ integrates tissue damage- and microbe-induced signaling

$cPla_2$ has been reported as key effector of osmotic tissue damage induced cell swelling for triggering zebrafish innate immune inflammatory responses (Enyedi et al., 2013, 2016). In line with those previous studies, knocking down of $cPla_2$ with different morpholinos decreased neutrophil recruitment against PA infection under hypotonic bating condition in fish larvae, while overexpression of *cpla*$_2$ by mRNA injection increased neutrophil responses (Figure 2.6A, B, D). Furthermore, ear injection of arachidonic acid, the product of $cPla_2$ enzymatic activity, induced neutrophil recruitment in the absence of tissue osmotic damage signaling (Figure 2.4A, B). Downstream of $cPLA_2$, cyclooxygenases (COX) and 5-lipooxygenase (5-LOX) metabolize arachidonic acid into lipid chemoattractants, e.g. prostaglandins, oxo-eicosanoids, and leukotrienes (Dennis and Norris, 2015; Rådmark et al., 2015). Fish larvae treated with Zileuton, the 5-LOX inhibitor, and Licofelone, the 5-LOX/COX dual inhibitor, showed attenuated neutrophil recruitment. Asprin, a COX inhibitor, did not block neutrophil recruitment-if anything, we noticed stimulation, likely due to the shunting effect of more AA into the 5-LOX pathway (Figure 2.4A, B). Together with our previous work (Enyedi et al., 2013, 2016), this suggests that the osmotic damage cues during microbial infection activate the 5-LOX branch of eicosanoid cascade, which generates potent neutrophil chemoattractants, such as 5-oxo-ETE and leukotrienes B4 (LTB_4).

Figure 2.6 $cPla_2$ integrates tissue damage and microbial cues.

(A) Summary of genetic pathway perturbations (indicated below the graph). Two measurements are given: the HR-index (red, pie charts), and average leukocyte recruitment curves (orange circles, simplified 3-timepoint-plot format: 0', 45', 90', see Figure 4.1). Upper graph section, color code indicates respective bathing conditions. Lower graph section, color code indicates injection conditions. Note, the injection buffer tonicity is always the same as bath tonicity. Error bars, SEM. Parentheses, aggregated number of animals per condition. Red lines, Fisher's exact test $p<0.05$. Orange lines, t-test $p<0.05$ (comparison of average leukocyte numbers at 90'). $cPla_2$ wt mRNA, $cPla_2$ overexpression by injection of mRNA into one-cell stage embryos. $cPla_2$ S498A mRNA, $cPla_2$ phosphorylation site mutant overexpression by injection of mRNA into one-cell stage embryos. *cpla₂* MO, published splice blocking morpholino (Enyedi et al., 2013). *fleN* mutant PA (multi-flagellated), ear injection of a flagella mutant of PA (Feinbaum et al., 2012). LPS mutant PA, ear injection of O-antigen mutated PA (ORF_11) (Feinbaum et al., 2012). *myd88* MP MO, misprime control morpholino. *myd88* MO, published translation blocking myd88 morpholino (van der Sar et al., 2006). Note, the Hypo + PA reference set is the same as in other figures. (B) Average neutrophil recruitment to PA-injected ears in the presence of osmotic tissue damage signals and $cPla_2$ knockdown (red & magenta) by two additional morpholinos. Note, the aggregated Hypo + PA data set (black) is the same as in other figures. (C) Average neutrophil recruitment to PA-infected ear upon *pycard* antisense knockdown. Shaded area, SEM of n animal experiments. Note, aggregated reference data set (Hypo + PA) is the same as in all other figures. Inset, *pycard* splice morphant confirmation by RT-PCR. Morphants show a 548 bp insertion. (D) Morpholinos reduce $cPla_2$ protein levels as confirmed by western blot. (E) Anti-$cPLA_2$ and anti-β-actin western blots of phospho-affinity column eluate (EL) and flow through (FT) at indicated experimental conditions. Note, unspecific β-actin signal (~23 kD) confirms equal gel-loading. Note, specific β-actin signal in flow through (~40 kD) confirms equal column-loading. M, colorimetric molecular size marker. Representative of two, independent experiments.

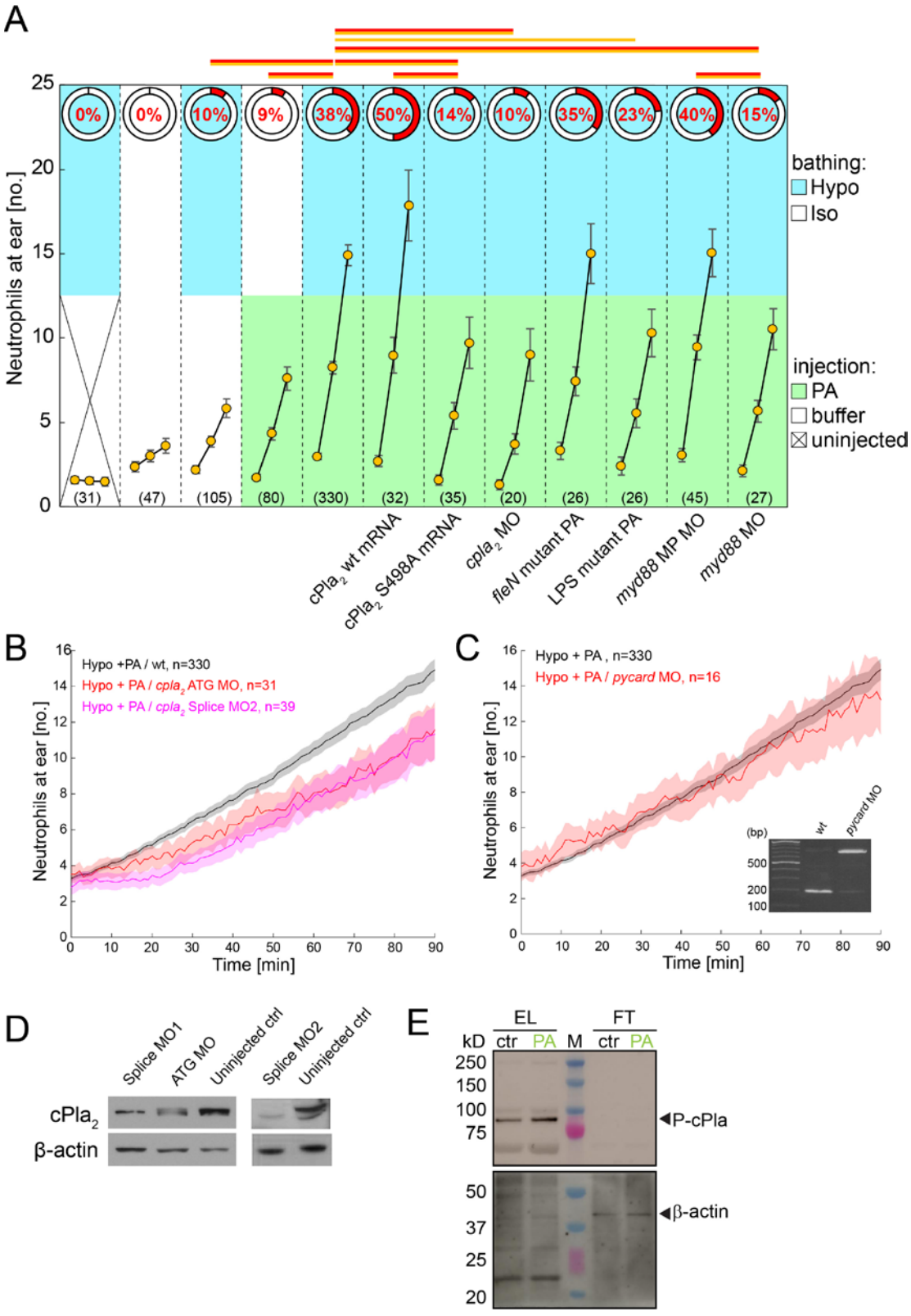
A
Neutrophils at ear [no.]
0%
0%
10%
9%
38%
50%
14%
10%
35%
23%
40%
15%
(31)
(47)
(105)
(80)
(330)
(32)
(35)
(20)
(26)
(26)
(45)
(27)
bathing:
Hypo
Iso
injection:
PA
buffer
uninjected
cPla2 wt mRNA
cPla2 S498A mRNA
cpla2 MO
fleN mutant PA
LPS mutant PA
myd88 MP MO
myd88 MO
B
Hypo +PA / wt, n=330
Hypo + PA / cpla2 ATG MO, n=31
Hypo + PA / cpla2 Splice MO2, n=39
Neutrophils at ear [no.]
Time [min]
C
Hypo + PA , n=330
Hypo + PA / pycard MO, n=16
Neutrophils at ear [no.]
Time [min]
(bp)
wt
pycard MO
500
200
100
D
Splice MO1
ATG MO
Uninjected ctrl
Splice MO2
Uninjected ctrl
cPla2
β-actin
E
EL
FT
kD
ctr
PA
M
ctr
PA
250
150
100
75
P-cPla
50
37
25
20
β-actin

As our mRNAseq data indicated that PA were likely detected through LPS signaling, we tested the involvement of LPS by infecting zebrafish larvae with a LPS-mutant PA strain (Feinbaum et al., 2012). Indeed, leukocyte recruitment to LPS-mutant PA strain was markedly reduced, whereas a multi-flagellated PA strain (PA *fleN*) (Feinbaum et al., 2012) did not alter the neutrophil responses (Figure 2.6A). As LPS is recognized by TLR signaling pathways in mammals (Barton and Medzhitov, 2003), we set out to test whether knocking down of MyD88, a conserved TLR adaptor protein involved in LPS recognition in zebrafish (van der Vaart et al., 2013), would reduce neutrophil recruitment. Indeed, upon PA infection, neutrophil recruitment was attenuated in the fish treated with published *myd88* morpholino compared to *myd88* mismatch morpholino control (van der Sar et al., 2006) (Figure 2.6A). This is consistent with the notion that PA is detected, at least in part, through LPS signaling. Previous study has shown that LPS can also be recognized through noncanonical inflammasomes, which trigger IL-1 signaling (Kayagaki et al., 2013). However, morpholino knockdown of Pycard (ASC), a conserved inflammasome adaptor, had little effect on early neutrophil recruitment (Figure 2.6C).

PA LPS is known to induce phosphorylation of $cPLA_2$ through a LPS-TLR-MyD88-MAP kinase signaling cascade (Hurley et al., 2006, 2011; Lindner et al., 2009; Qi and Shelhamer, 2005; Ruipérez et al., 2009), and $cPLA_2$ phosphorylation augments the enzyme's hydrolytic activity, which unfolds after membrane attachment (Tucker et al., 2009). In line with others, we previously reported that phosphorylation does not increase membrane recruitment of $cPla_2$ (Enyedi et al., 2016; Schievella et al., 1995;

Tucker et al., 2009). Instead, $cPla_2$ membrane interactions are stimulated by Ca^{2+} and nuclear membrane stretch, which are both induced by tissue damage (Enyedi et al., 2016). As phosphosite-specific antibodies for zebrafish $cPla_2$ are not available, we set out to detect stimulation of $cPla_2$ phosphorylation upon ear infection by affinity purification of phosphoproteins from larval extracts. Indeed, an increase of $cPla_2$ phosphorylation was detected upon PA infection (Figure 2.6E). It is worth noting that these whole-animal phosphorylation changes underestimate local phosphorylation increase at ear infection site. Furthermore, by mutating $cPla_2$`s primary, conserved phosphorylation site (S498A), and injection of the S498A mutant mRNA, we observed strongly decreased neutrophils recruitment against PA infection (Figure 2.6A), which confirmed that $cPla_2$ phosphorylation controlled antimicrobial neutrophil responses *in vivo*. Additionally, zebrafish treated with U1026, the inhibitor of Erk1/2 pathway, but not SB203580, the inhibitor of p38 pathway, showed attenuated neutrophil response upon ear infection (Figure 2.7A, B), which is in line with previous study (Zhu et al., 2002). Taking together, these experiments indicate that $cPla_2$ mechanochemically integrates microbe and tissue damage cues (Figure 2.7C).

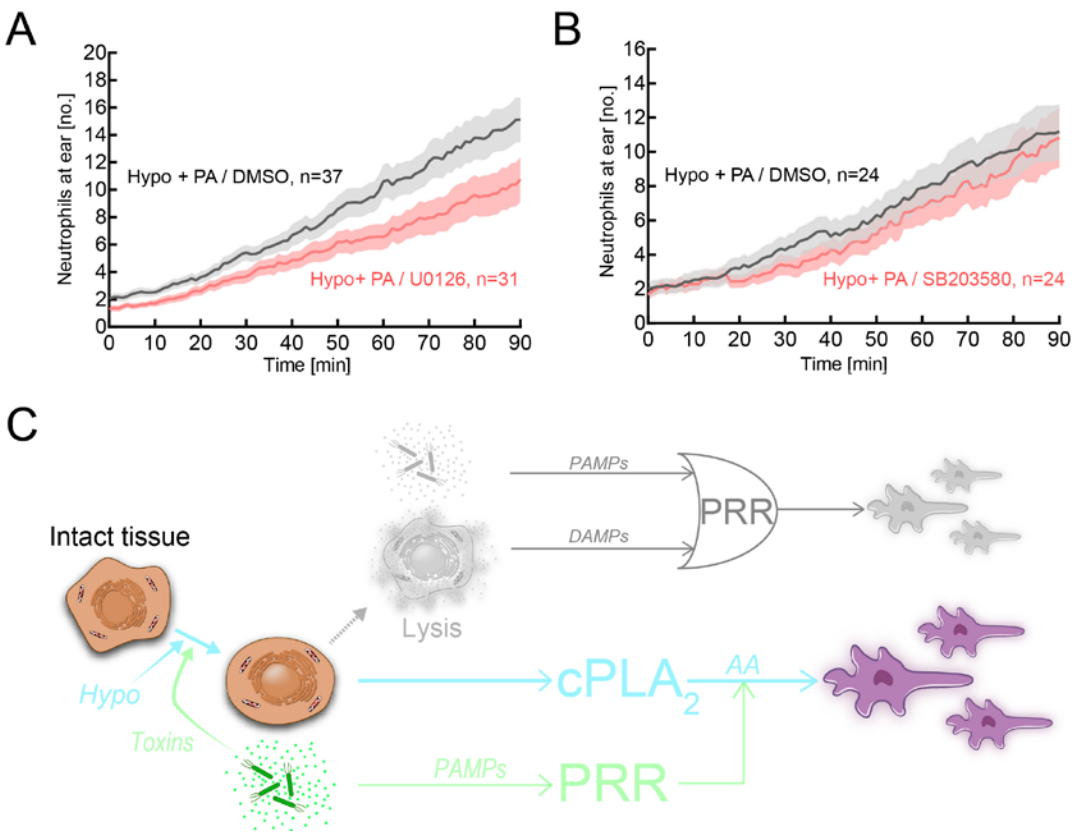

Figure 2.7 Scheme of proposed experimental model.

(A) Average neutrophil ear recruitment to PA upon U0126 treatment. Shaded area, SEM of n injection experiments. (B) Average neutrophil ear recruitment to PA upon SB203580 treatment. Shaded area, SEM of n injection experiments. (C)Regulatory diagrams juxtaposing the classical view(upper panel, muted colors) of inflammation initiation with the model supported by this study (lower panel). Classically, *either* PAMPs released by microbes *or* DAMPs released by lytic host cells are thought to function as primary triggers for inflammation and leukocyte recruitment. The logical OR relationship is depicted by its standard symbol in the upper diagram. Our study suggests that only tissue damage can function as primary, inflammatory trigger *in vivo*, and that microbial signals act as amplifiers of tissue damage signaling. Depicted on the left side is the necrotic sequence of cell morphology changes. Arrows mark the proposed regulatory role of each necrotic intermediate. Whereas classic DAMP signaling is triggered by cell lysis, the tissue damage signaling pathway proposed in this study is triggered upstream of lysis by cell- and nuclear swelling. Note that necrotic cell lysis causes strong additional nuclear swelling through extranuclear colloid osmotic pressure drop, which can further activate nuclear $cPla_2$ (Enyedi et al., 2016). For simplicity, this post-lytic nuclear swelling is omitted from the diagram. PAMP, pathogen associated molecular pattern. DAMP, damage associated molecular pattern. PRR, pattern recognition receptor. $cPLA_2$, cytosolic phospholipase A_2. AA, arachidonic acid.

Chapter III: Discussion

In our study, we blocked tissue damage signaling in the context of bacterial infection, for the first time to our knowledge in any *in vivo* model organisms. Surprisingly, tissue damage signaling turned out to be essential for antibacterial inflammatory response. Although bacterial signals were still detected, they triggered little-to-none neutrophil recruitment.

Such result may be due to the molecular activation mechanism of $cPLA_2$. Bacterial signals induce the phosphorylation of $cPLA_2$. However, the resulting augmentation of the hydrolytic activity of $cPLA_2$ will not impinge on the production of proinflammatory eicosanoids until the enzyme meets its substrate on membrane. As the primary step of $cPLA_2$ activation, translocation of $cPLA_2$ requires Ca^{2+} influx and mechanical stretch of the nuclear membrane, which are selectively induced by tissue damage. This may explain why *E. coli* and PA *exoU* triggered little-to-none neutrophil recruitment under isotonic bathing condition (HR_i=0% and HR_i=2%, respectively, Figure 2.2B), which is lower than the neutrophil recruitment induced by tissue damage alone (HR_i=10%, Figure 2.6A). Although we demonstrated some "virulence factors", e.g. ExoU, are able to induce neutrophil responses on their own, it is not deniable that *E. coli* and PA *exoU* still possess a wide range of PAMPs. Thus, their inability to trigger innate immune responses contests the wide spread assumption that both PAMPs and DAMPs can attract leukocytes as they share the same PRRs (Table 1.1).

Two-signal (or co-stimulation) models have been well studied in adaptive immunity as a regulatory scheme to ensure specificity. For example, T cells are only activated upon receiving of two distinct cues: the primary antigenic signal and the second co-stimulatory protein contact between T cell and the antigen presenting cell (APC) (Matzinger, 2002; Vance, 2000). Additionally, the production of mature Il1β also requires initial NF-κB signaling to initiate the synthesis of pro- Il1β protein, and inflammasome signaling to activate caspase-1, which processes pro-Il1β into its active form (Netea et al., 2010). Although adaptive immunity is absent in zebrafish larvae, a two signal model for $cPla_2$ activation emerges from our study.

Besides inducing the translocation of $cPLA_2$, cell swelling is also known to trigger activation of inflammasome (Compan et al., 2012; Muñoz-Planillo et al., 2013). Moreover, previous studies have also demonstrated LPS can activate inflammasome in a nonconanical manner (Shi et al., 2014). However, neither blocking protein synthesis (Figure 2.4A,B), nor knocking down of Pycard (Figure 2.6C), a conserved inflammasome adaptor (Gross et al., 2011), affected neutrophil responses. These data exclude the involvement of inflammasome in our system.

Our study also provide a potential explanation for the long-standing question about how our immune system discriminate the commensal bacteria from virulent pathogens (Bäckhed et al., 2005; Nathan, 2006). However, such speculation demands more follow-up research. Nevertheless, our results provide a compelling rational for

the conundrum of why sterile inflammatory signaling evolved in the first place: to mediate rapid neutrophil response to epithelial infection.

One of the questions left unanswered in our study is the phenotypic heterogeneity (i.e. high responders versus low responders) of neutrophil recruitment in microbial infected zebrafish larvae. As discussed previously, we speculate the cause could be either technical (e.g. the stochasticity of injection-induced ear rupture) or biological (e.g. (epi-)genetic variability). To test the potential contribution of technical factors, a titration of injection volume can be utilized to intentionally induce more or less ear rupture along with the same microbial infection burden. Such involvement will be confirmed if HR_i correlates with injection volume. To test the potential contribution of biological factors, a group of zebrafish larvae infected under the same condition can be first sorted out based on their neutrophil recruitment pattern (i.e. high or low responders) under microscope, followed by DNA/RNA sequencing analysis of different groups of infected larvae.

Another immediate follow-up experiment could focus on figuring out in which cell type that $cPla_2$ mainly functions. To address the involvement of different cell types, a morpholino dependent cell depletion strategy can be utilized as previously reported (Palha et al., 2013). Alternatively, one could also express a dominant negative *cpla*$_2$ mutant (e.g. *cpla*$_2$ S498A) in a cell type specific manner. Such experiment is important because it can provide the target information for the potential therapeutic treatment of sterile inflammation induced diseases.

Chapter IV: Materials and methods

General fish procedures

Adult wt and transgenic reporter casper (White et al., 2008) zebrafish, and larvae were maintained according to institutional animal healthcare guidelines as described (Nüsslein-Volhard and Dahm) with the approval of the Institutional Animal Care and Use Committee (IACUC). For injection assays, 2.5-3 days post-fertilization (2.5-3 dpf) larvae were anaesthetized in E3 medium (5 mM NaCl, 0.17 mM KCl, 0.33 mM $CaCl_2$, 0.33 mM $MgSO_4$) containing 0.2 mg/mL ethyl 3-aminobenzoate methanesulfonate (Sigma).

Widefield fluorescence imaging

For all imaging experiments, transgenic, transparent (TG(*lysC*:Casper1GR), casper background) zebrafish larvae expressing TagRFP in neutrophils were embedded in 1% low melting (LM) agarose (Gold Biotechnologies) and maintained in standard, hypotonic E3, or isotonic E3 medium (that is, standard E3 supplemented with 140 mM NaCl), containing the indicated compounds. Every minute, starting at ~10-15 min post injection, images were acquired. TagRFP and FluoSphere fluorescence were excited with an LED light source (Lumencor) using 549/15 and 438/24 bandpass filters, respectively, together with a multispectral dichroic (59022 bs, Chroma). Both TagRFP fluorescence, and the red tail of the FluoSphere emission was acquired with a 632/60 emission filter (Chroma). Fluorescence of EGFP-tagged PA was excited using a 475/28 bandpass filter together with a multispectral dichroic (59022 bs,

Chroma), and acquired using a 525/50 emission filter (Chroma). Images were captured at room temperature (~25 °C) using NIS-Elements (Nikon) on an Eclipse Ti microscope (Nikon) equipped with a 10x plan-apochromat NA 0.45 air objective lens, a Clara CCD camera (Andor), and a motorized stage.

Plasmid construction

The TG(*lysC*:Casper1GR) transgenic line was created using the Tol2kit system as previously described (Kwan et al., 2007), by recombining the *lysC* promoter (Hall et al., 2007), full-length Casper1GR (that is, a TagGFP and a TagRFP connected by a YVAD motif, originally developed as FRET-sensor for caspase activation (Liu et al., 2014) and here used as fluorescent neutrophil marker), and a SV40 polyadenylation sequence into to the pDestTol2CG2 vector backbone.

pCS2+cPla$_2$mKate2 for cPla$_2$ overexpression by mRNA injection was generated as previously described (Enyedi et al., 2016). Serine-to-Alanine mutation at position 498 (S498A) was achieved using the QuikChange Lightning Site-Directed Mutagenesis Kit (Agilent). Primers used for mutagenesis were: forward, 5'-TCAACCCTGCCCTTCGCTCCCTTCAGCGGCATC – 3'; reverse, 5' – GATGCCGCTGAAGGGAGCGAAGGGCAGGGTTGA – 3' (Enyedi et al., 2016). Sequencing confirmed the mutation.

Generation of transgenic lines

A solution containing the *lysC*:Casper1GR transgene plasmid and transposase mRNA was injected into the cytosol of one-cell stage casper embryos. Injected larvae with mosaic cardiac EGFP (enhanced green fluorescent protein) expression were raised to sexual maturity and screened by crossing to wt fish to identify founders. Founders were crossed to wt caspers, or subsequent F1 transgenic siblings were crossed together to obtain the 2.5-3 dpf transgenic larvae used in the ear infection experiment.

Bacterial strains and growth conditions

Wild-type, and EGFP-tagged *Pseudomonas aeruginosa* (strain PA14) were generously provided by Dr. Joao Xavier (MSKCC, New York, NY). PA14 mutant strains ORF_11, *fleN, and exoU* (Feinbaum et al., 2012) were generously provided by Dr. Cole Haynes (University of Massachusetts Medical School, Worcester, MA). One Shot TOP10 chemically competent *E. coli* (Thermo Fisher) were used as nonpathogenic bacteria. Wt PA14 and *E. coli* liquid culture was grown in pure LB medium. Mutant PA strains were cultured in LB medium containing 15 µg/mL Gentamycin (IBI Scientific). All cultures were incubated at 37℃ in a rotary shaker at 250 rpm. Heat-killed PA14 were prepared by heating the bacteria at 65℃ for 1 h (Matsumoto et al., 1998).

Bacterial infection through ear or muscle injection

Bacteria were resuspended in either E3 or isotonic E3 medium, and the optical density was measured at 600 nm with a Ultraspec 10 cell density meter (Amersham Biosciences). To prepare the final inoculum, the bacteria suspension was diluted or

pelleted by centrifugation at 1800xg for 10 min, followed by resuspension to achieve the desired bacterial density (OD_{600}=7). Fluorescent beads (Blue-green FluoSpheres, Life Technologies) were added to the bacterial aliquots prior to injection for a final ratio of 1:1. Ear injection was performed as previously described (Deng et al., 2012). Muscle injection was performed by injecting bacteria into the segmented muscle above the yolk extension. Injections were performed using a Nanoject II microinjector (Drummond Scientific). After bacterial infection, a serial-diluted inoculum was plated to quantify colony forming units (CFU). The volume of inner ear was estimated by approximating the ear vesicle as a sphere, and measuring its radius.

Survival assay

2.5-3 dpf zebrafish larvae were injected with serial-diluted PA suspended in either E3 or isotonic E3 medium. Larvae injected with isotonic suspension were kept in isotonic E3 fish bathing solution for 2 h before transferring them back to standard, hypotonic E3 bathing solution. Larval viability was monitored for 5 days after injection. Dead larvae were scored by loss of tissue transparency and heartbeat.

Image processing and data analysis

Leukocyte recruitment to the ear and muscle was computationally measured by counting neutrophil number within the ear or muscle region per frame for 90 min (1 min/frame for ear injections, and 2.5 min/frame for muscle injections). Time-lapse movies were background subtracted using the MOSAIC background subtractor plugin

(Sbalzarini and Koumoutsakos, 2005) (http://mosaic.mpi-cbg.de/?q=downloads/imageJ) in ImageJ/FIJI (Schindelin et al., 2012). All images of the background-subtracted time-lapse movies were maximum intensity projected (11 z-planes per frame, 8 µm per z-step) using ImageJ/FIJI. The ear vesicle outlines were detected based on dispersed bead fluorescence. To define the infection-area/region of interest (ROI) after muscle injection, all image filenames were blinded in CellProfiler (Lamprecht et al., 2007), and the approximate needle injection site as marked by bead fluorescence was manually outlined as ROI. We used two different computational methods to count fluorescent neutrophils in the ear, whose accuracy and suitedness we initially confirmed through manual measurements. When neutrophils did not visibly aggregate into large clusters, we used local fluorescence intensity maxima detection (implemented in a Python script, Anaconda distribution) for determining the position and number of leukocytes within an image. Because neutrophil cluster formation posed a challenge for detecting individual leukocytes by local maxima detection, we analyzed time-lapse movies with neutrophil clusters using a custom analysis pipeline in CellProfiler (Lamprecht et al., 2007) and Matlab (MathWorks). Briefly, average neutrophil fluorescent intensity was estimated from the first 10 frames of each time-lapse movie. Neutrophil numbers were then determined by dividing total neutrophil fluorescence intensity of the ear by averaging neutrophil fluorescence. Visual inspection confirmed that this method more accurately estimated leukocyte numbers in the presence of clustering than local maxima detection. To approximate neutrophil numbers within the muscle ROI, the above described CellProfiler pipeline and manual counting methods were applied depending on

whether neutrophils formed visible aggregates. For clearer data presentation in Figure 2.4A and 2.6A, a segmented line fit was used to represent average leukocyte recruitment kinetics within the first (0-45 min) and second half (46-90 min) of each time-lapse movie (Figure 4.1). The number of high responders in each experimental condition was computationally identified: Neutrophil response curves were blindly selected from a total pool of 1600 experiments across 41 experimental conditions, including those reported in the manuscript, and manually classified into representative high and low responders training sets (with 40 curves per set). The Euclidian distance of leukocyte recruitment curves to the median of the two training sets (Matlab 'pdist2' command) was calculated. Curves more similar to the median of the high responder training set than to the median of the low responder training set were computationally classified as "high responders", and vice versa. User-unsupervised, Gaussian mixture distribution model clustering (McLachlan and Peel, 2000) into two clusters using the Matlab 'fitgmdist' command gave largely similar results (Figure 2.4B). In this fully automated method, all available leukocyte recruitment curves (from 1813 individual injection experiments at that time, including those described in the figures) were used to generate the two-component Gaussian mixture distribution model.

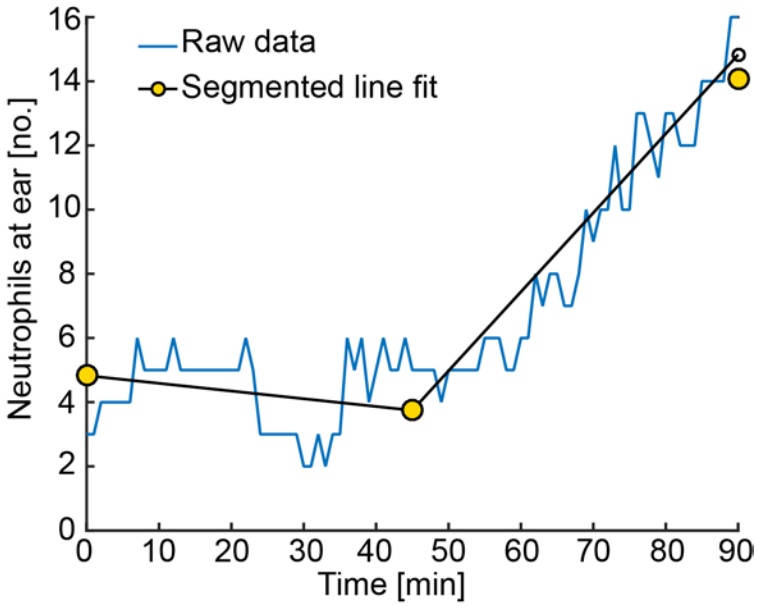

Figure 4.1 Segmentation of average time-lapse recruitment curves into a simplified 3-point recruitment curves with error bars as presented in Figure 2.4 A and 2.6 A.

Leukocyte trajectory analysis

Trajectory analysis was carried out on a subset of the time-lapse movies used for computational quantification of neutrophil recruitment to the ear (see above). Trajectories were manually generated using the MTrackJ plugin of ImageJ/FIJI (Meijering et al., 2012). The ear region was identified by dispersed bead fluorescence, or by transmitted light morphology as appropriate. Leukocytes that were <100 µm away from the ear outline in the first frame were followed by manual tracking. Average migration velocity (v), path length (l), and path directional persistence (D_p) were calculated as previous described (Enyedi et al., 2013).

mRNA preparation and injection

For the $cPla_2$ or $S498AcPla_2$ overexpression experiments (Figure 2.6A), pCS2+$cPla_2$mKate2 or pCS2+$cPla_2$S498AmKate2 were linearized, and *in vitro* transcribed using the mMessage mMachine SP6 kit (Thermo Fisher). 2.3 nL of 500 ng/µL mRNA was injected into one-cell stage zebrafish embryos.

Pharmacological treatments

Larvae were preincubated for 40-60 min in E3 or isotonic E3 supplemented with the following compounds: 20 µM Zileuton (Cayman), 100 µM Aspirin (Acetylsalicylic acid, ACROS Organics), 50 µM Licofelone (Cayman), 400 µg/mL cycloheximide (CHX, Sigma), 100 µM U0126 (Cell Signaling Technology), 100 µM SB203580 (Cell Signaling Technology). 0.5% digitonin (Cayman) and 120 µM melittin (Millipore) were injected into the ear without preincubation. 25 µM arachidonic acid (Sigma) was injected into the ear, and simultaneously applied in the bathing solution. Dimethyl sulfoxide (DMSO, Sigma) was used as a solvent for all water non-soluble compounds with a maximal concentration of 1%. Isotonic E3 was used to dissolve digitonin and melittin. Compounds were present throughout the experiments. To confirm the inhibitory efficiency of CHX, 2.5-3 dpf TG(*hsp70*: $cPla_2$mKate2) (Enyedi et al., 2016) zebrafish were pretreated with 400 µg/mL CHX or 0.1% DMSO for 1 h at 28℃ followed by 1 h heat shock at 37℃. Heat shock-induced expression of mKate2 fluorescence was measured over 5 hours by fluorescence microscopy (Figure 4.2).

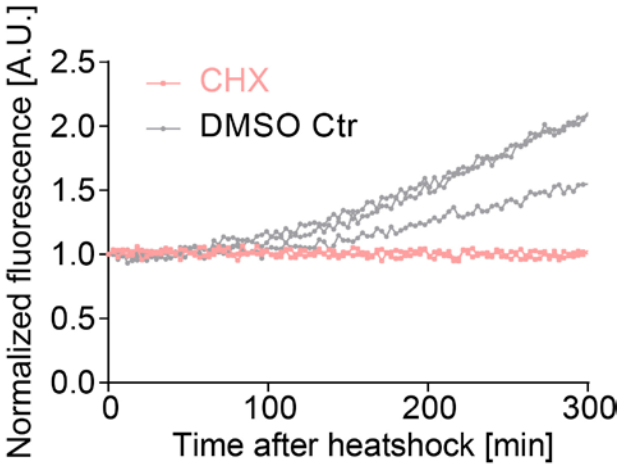

Figure 4.2 3 dpf TG(*hsp70*:cPla$_2$mKate2) fish larvae were pretreated with CHX or DMSO control for 1 h at 28ºC followed by 1 h heat shock at 37°C. Larvae were imaged for 5 h to measure protein expression via mKate2 fluorescence. Individual curves denote the fluorescence signal within an individual animal.

Antisense morpholinos

One-cell stage embryos were injected with 2.3 nL morpholino (Gene Tools) diluted in water. With one exception, only previously characterized morpholinos were used (Enyedi et al., 2013; Progatzky et al., 2014; van der Sar et al., 2006):

Table 4.1 Applied morpholinos.

Name	Sequence	Type	Amount/embryo (picomole)	Ref.
cpla$_2$ MO1	5'- AAGCGTCACTTACTATAATGTTGGA-3'	Splice	2.3	Enyedi et al., 2013
cpla$_2$ MO2	5'-TCCCTTTTAGAATTTACCTTGCCGA-3'	Splice	1.2	This paper
cpla$_2$ ATG	5'-ATGCTCAACTATAATGTTGGACATT-3'	ATG	2.3	Enyedi et al., 2013
pycard MO	5'-CAATTGCACTTACATTGCCCTGTGT-3'	Splice	1.2	Progatzky et al., 2014

Table 4.1 (Continued).

myd88 MO	5'-TAGCAAAACCTCTGTTATCCAGCGA-3'	ATG	0.6	Van der Sar et al., 2006
myd88 MP	5'-TAcCAtAACCTgTGTTATCgAGgGA-3'	Misprime	0.6	Van der Sar et al., 2006

$cPla_2$ knockdown was confirmed SDS-PAGE and western blotting of morphant/control lysates using a zebrafish cross-reactive $cPLA_2$ antibody (Abcam; 1:500). To confirm knockdown with the *pycard* MO, morphant mRNA was isolated from 2.5-3 dpf larvae with Oligo $(dT)_{25}$ Dynabeads (Invitrogen), followed by one-step RT-PCR using RevertAid First Strand cDNA Synthesis Kit (Thermo Scientific). Primer sequences were as follows: *pycard* forward, 5' - CGCGTCACAAAGTCTGCAAT-3'; *pycard* reverse, 5' - CATCAGAGGGAGCACCTTTGC-3' (Progatzky et al., 2014).

SDS-PAGE and western blotting

2.5-3 dpf larvae were anaesthetized and homogenized in RIPA buffer (Cell Signaling Technology) supplemented with 1x cOmplete protease inhibitor cocktail (Roche). Homogenization was performed for 45 s in a FastPrep 24 Cell Disrupter (MP Biomedicals) at maximum speed (6.5 m/s) in the cold room. Protein concentration was quantified by standard bicinchoninic acid assay (BCA) assay. Equal amounts of protein were separated by NuPAGE 4%-12% Bis-Tris gel electrophoresis according to the manufacturer's protocol (Life Technologies), and wet-transferred to a nitrocellulose membrane in Tris-Glycine transfer buffer containing 20% methanol at

120 V for 90 min at 4℃. Western blot membranes were probed with anti-cPLA$_2$ (Abcam; 1:500), and anti- β-actin (SIGMA-ALDRICH; 1:5000) primary antibodies, followed by incubation with goat anti-rabbit IgG-HRP (Santa Cruz Biotechnology; 1:5000) and goat anti-mouse IgG-HRP (Santa Cruz Biotechnology; 1:5000), respectively. Amersham ECL prime western blotting detection reagent (GE Healthcare) was used for western band detection according to manufacturer`s protocol. Chemiluminescence detection was performed with an ImageQuant LAS 500 device (GE Healthcare).

Measuring cPla$_2$ phosphorylation in larval lysates by affinity purification

Phosphorylation-specific antibodies are not available for zebrafish cPla$_2$. To determine the levels of phosphorylated cPla$_2$ in infected zebrafish larvae, we instead resorted to an affinity purification scheme. At least 30 fish were injected with standard E3 with/without PA (OD_{600}=7) as described above. Phosphorylated proteins were isolated using PhosphoProtein Purification Kit (Qiagen) according to manufacturer's protocol with three modifications: (i) 1X PhosSTOP phosphotase inhibitor (Roche) was added to PhosphoProtein lysis buffer. (ii) Fish were homogenized with FastPrep 24 Cell Disrupter as described above. (iii) Fish tissue homogenate was diluted in 300 µL lysis buffer. The column eluate was concentrated to <50 µL using Nanosep Ultrafiltration Columns from the kit. Western blotting analysis was performed as described above. To confirm equal lysate-loading onto the phospho-affinity column, the column flow-through (FT, Figure 2.6 E) was analyzed by SDS-PAGE and western blotting using an anti-β-actin antibody.

Embryo collection, RNA extraction and sequencing

PA resuspended in either standard or isotonic E3 were injected into the otic vesicle of 2.5-3 dpf zebrafish larvae. Uninjected zebrafish larvae served as control. ~20 larvae from each group were euthanized 1 h after injection. After homogenization, total RNA was extracted using Trizol reagent (Life technologies) according to manufacturer`s protocol. The following procedures were performed by the MSKCC Genomics and Bioinformatics core facilities. Briefly, after Quant-It quantification and quality control of Agilent BioAnalyzer, 500 ng of total RNA underwent polyA selection and Truseq library preparation according to instruction provided by Illumina (TruSeq Stranded mRNA Library Prep Kit), with 8 cycles of PCR. Samples were barcoded and run on a Hiseq 2500 in a 50bp/50bp Paired end run, using the TruSeq SBS Kit v4 (Illumina). An average of 42 million paired reads was generated per sample. The percent of mRNA bases was close to 53% on average. The output data (FASTQ files) were mapped to the zebrafish genome GCz10 (UCSC) using the rnaStar aligner (Dobin et al., 2013) that mapped reads genomically and resolved reads across splice junctions. A two pass -mapping method (Engström et al., 2013) was used in which the reads were mapped twice. The first mapping pass used a list of known annotated junctions from Ensemble. Novel junctions found in the first pass were then added to the known junctions, and a second mapping pass was done (on the second pass the RemoveNoncanoncial flag was used). After mapping, the output SAM files were post processed using the PICARD tools to: add read groups, AddOrReplaceReadGroups which in additional sorted the file and converted it to the

compressed BAM format. The expression count matrix was then computed from the mapped reads using HTSeq (www-huber.embl.de/users/anders/HTSeq). The raw count matrix generated by HTSeq were then be processed using the R/Bioconductor package DESeq (www-huber.embl.de/users/anders/DESeq), which was used to both normalize the full dataset and analyze differential expression between sample groups.

Whole mount *in situ* hybridization (WISH)

To generate the *il1b* antisense riboprobe, probe template was amplified from zebrafish cDNA by PCR with a T7-modified antisense primer (Forward, 5'-ATGGCATGCGGGCAATAT-3', reverse, 5'-TAATACGACTCACTATAGGGCTGCAGCTCGAAGTTAATGATG-3') and was transcribed *in vitro* with T7 polymerase with conjugated Digoxigenin-11-uridine-5'-triphosphate (DIG-11-UTP) from DIG RNA Labeling Kit (T7) (Roche).

WISH was performed as previously described (Gerlach and Wingert, 2014). Briefly, ~ 20 2.5-3 dpf TG(*lysC*:Casper1GR) larvae were fixed in 4% paraformaldehyde (PFA, Aldrich) overnight at 4 °C. Following removal of PFA, larvae were washed two times with 1X PBST (1X PBS (Sigma), 0.1 % Tween-20 (Sigma)) followed by a wash with 100% methanol (Fisher) at room temperature. Larvae were first immersed in fresh 100% methanol for 20 min at -20 °C, then subsequently washed with 50% and 30% methanol (in PBST), and finally with PBST without methanol. Larvae were permeabilized with 10 µg/mL proteinase K (Roche, diluted in PBST) for ~22 min, and rinsed twice with PBST. Larvae were stored in 4% PFA overnight at 4°C. PFA was removed, and larvae were washed three times with PBST, and transferred to flat

bottom microcentrifuge tubes (Fisher Scientific). Following removal of PBST, larvae were incubated in 1 mL HYB+ hybridization solution (50% formamide (AmericanBio), 5x SSC (AmericanBio), 0.1% Tween-20, 5 mg/mL yeast torula RNA (Sigma), 50 µg/µL heparin (Sigma-Aldrich)) for 4 h at 70 °C. After HYB+ was removed, 500 µL 1 ng/µL *il1b* probe diluted in HYB+ was added, and larvae were incubated overnight at 70°C. Larvae were washed at 70 °C with 50% formamide/2X SSCT (2X SSC, 0.1% Tween-20) for 30 min (twice), for 15 min with 2X SSCT, and for 30 min with 0.2X SSCT (twice). Larvae were then washed twice in MABT (Maleic Acid Buffer: 0.1 M maleic acid (Sigma-Aldrich), 0.15 M sodium chloride (Fisher), 0.23 M Trizma base (Sigma), 0.1% Tween-20, pH=7.4) for 5 min at room temperature. Larvae were incubated in blocking solution (2% BSA (Sigma), 10% FBS (Corning), 70% MABT) for 2 h at room temperature. Anti-Digoxigenin (Anti-DIG) secondary antibody (Roche, 1:5000) recognizing DIG conjugated to alkaline phosphatase was applied at 4 °C overnight. To remove extra secondary antibody, larvae were quickly washed three times in MABT, followed by twelve 15 min washes in MABT. Colorimetric substrates of NBT (Sigma) and BCIP (Sigma) were applied to the larvae to generate a colorimetric signal. This reaction was monitored every 20 min to prevent background-overstaining and stopped at ~90 min by washing in PBST and subsequent fixation in 4% PFA. Larvae were mounted in glycerol (Sigma) for colorimetric imaging. Images were acquired with on stereo microscope (Nikon) equipped with a Nikon DS-Fi1 CCD color camera (Nikon).

Statistics

All error bars indicate standard errors of means (SEM). For most mean value comparisons, p-values were derived by unpaired, two-tailed t-tests assuming unequal variances (heteroscedastic) using Prism (GraphPad), Excel (Microsoft), or MatLab. For mean value comparison of tracking parameters in Figure 2.3 A, a one-way Anova test was applied (MatLab). For comparison of HR-indices, a two-tailed Fisher's exact test (Minitab) was used. For comparison of Kaplan-Meier survival curves, a log-rank test (Minitab) was used. For statistical analysis, animal experiments from different experimental days were aggregated. Sample sizes were not predetermined. The experiments were not randomized, and the investigators were not blinded to allocation during experiments or outcome assessment. A detailed summary of experimental numbers is provided (Table 5.3).

Chapter V: Appendix

Table 5.1 Differentially expressed genes: Hypo+PA versus Uninjected (log2 fold change>1).

GeneID	GeneSymbol	P.adj	log2[HypoPA/Uninjected]	Mean_counts_Uninjected	Mean_counts_HypoPA
ENSDARG00000098700	il1b	6.19E-34	4.188975345	15.45954689	281.9707054
ENSDARG00000015355	fosl1a	8.26E-45	4.087388605	124.6841444	2119.521389
ENSDARG00000090873	ccl34a.4	0.000874	3.287946708	3.418485095	33.38906627
ENSDARG00000045190	ch25h	0.00011	2.950995955	6.247979549	48.31454555
ENSDARG00000077308	gpr84	4.27E-10	2.682837571	16.51162075	106.024025
ENSDARG00000069844	irg1	3.80E-06	2.609096474	13.85967749	84.56086651
ENSDARG00000037859	il11a	0.002579	2.479204161	8.128068156	45.32127867
ENSDARG00000098752	csf3b	0.009198	2.44650494	6.291083387	34.29231569
ENSDARG00000104773	junbb	3.09E-38	2.43042895	757.0860265	4081.100097
ENSDARG00000055751	fosb	8.47E-07	2.428997221	44.17252377	237.877429
ENSDARG00000003203	rhcga	2.26E-13	2.364906237	123.6758058	637.0777874
ENSDARG00000042725	cebpb	7.23E-57	2.300400435	1399.961965	6896.135236
ENSDARG00000074378	junba	7.24E-31	2.293574734	337.5447202	1654.878492
ENSDARG00000031683	fosab	6.68E-32	2.285609614	632.9198783	3085.927994
ENSDARG00000040284	si:dkey-79d12.5	1.73E-25	2.243120949	162.1388264	767.5977884
ENSDARG00000091234	CU019646.2	2.82E-24	2.217707877	127.3702976	592.4678059
ENSDARG00000010276	ptgs2b	6.15E-07	2.166714508	350.3841533	1573.223827
ENSDARG00000012789	plek2	1.17E-08	2.041176307	140.4109428	577.9047314
ENSDARG00000013598	tnfb	3.92E-06	2.032814514	25.8143546	105.6329518
ENSDARG00000042816	mmp9	4.50E-21	1.980255763	384.4702886	1516.977598
ENSDARG00000012395	mmp13a	6.97E-05	1.975301222	152.6924355	600.402429
ENSDARG00000091209	ucp3	0.000754	1.96846924	369.0529773	1444.298633

Table 5.1 (continued).

ENSDARG00000017653	rgs13	0.0002	1.920034803	22.65170795	85.72135397
ENSDARG00000077540	f2rl1.2	2.27E-11	1.911525267	175.2220061	659.1968007
ENSDARG00000099195	ier2	9.94E-21	1.8365397	510.1169189	1821.894672
ENSDARG00000089724	cyldb	0.006538	1.791878171	90.39623315	313.0108643
ENSDARG00000079922	klf4	8.57E-06	1.784397655	80.65377312	277.8317712
ENSDARG00000028396	fkbp5	0.008077	1.779316393	997.8920156	3425.3989
ENSDARG00000075045	cxcl18b	0.000303	1.74051999	44.20119364	147.7007575
ENSDARG00000078619	pnp5a	8.26E-45	1.688010764	2452.62222	7902.646062
ENSDARG00000087303	cebpd	6.17E-25	1.673470024	1652.91944	5272.497246
ENSDARG00000079497	C5H8orf4 (2 of 2)	5.97E-17	1.655342895	1116.627884	3517.356054
ENSDARG00000103980	ets2	1.70E-30	1.637840337	650.0500261	2022.953264
ENSDARG00000086881	IER2 (1 of 2)	5.87E-11	1.635885042	262.9954585	817.3324017
ENSDARG00000020133	jdp2b	7.89E-07	1.601588902	153.2273637	465.0103613
ENSDARG00000002353	tagapa	0.005146	1.543478714	34.24623537	99.82658805
ENSDARG00000094901	ABCC6	4.04E-10	1.528850995	99.78679683	287.9407226
ENSDARG00000058606	sik1	4.22E-06	1.527281019	3127.600719	9015.061688
ENSDARG00000088337	wu:fc34e06	4.58E-15	1.52427791	433.7420736	1247.627457
ENSDARG00000089156	egr3	5.29E-18	1.518615682	274.5299674	786.5722682
ENSDARG00000005673	f3b	0.000662	1.506691547	163.8020683	465.4561049
ENSDARG00000087732	Metazoa_SRP	0.000203	1.504082146	268.0310197	760.2543268
ENSDARG00000007823	atf3	2.82E-24	1.502403293	472.3231988	1338.159045
ENSDARG00000023217	crema	2.78E-15	1.446670318	355.3947023	968.7285722
ENSDARG00000075121	hbegfa	1.70E-30	1.446309358	961.4684633	2620.098048
ENSDARG00000001953	pfkfb3	0.009633	1.435248577	887.2057886	2399.259591

Table 5.1 (continued).

ENSDARG00000004539	ptgs2a	5.13E-28	1.430971505	832.2468063	2243.972256
ENSDARG00000013576	gadd45bb	2.43E-07	1.422707233	181.3642675	486.2160361
ENSDARG00000099351	igfbp1a	6.75E-11	1.407592729	789.9423542	2095.670659
ENSDARG00000100947	mafk	0.005923	1.399446932	58.24241679	153.6437476
ENSDARG00000055854	nr4a3	8.86E-22	1.398584593	491.7962223	1296.585326
ENSDARG00000099002	creb5a	0.001406	1.384791732	46.98949299	122.7056635
ENSDARG00000099411	zgc:158343	1.70E-13	1.377840668	498.802826	1296.284344
ENSDARG00000037861	slc2a3b	5.94E-05	1.361031856	98.23950641	252.3466742
ENSDARG00000002298	ankrd22	2.42E-06	1.353042955	86.51115116	220.9930449
ENSDARG00000020298	btg2	3.19E-13	1.334942652	1770.563731	4466.520633
ENSDARG00000035422	cyr61l1	0.000667	1.326570049	72.56951681	182.0084736
ENSDARG00000098837	tgm5l	0.022683	1.320812701	33.28368478	83.14490506
ENSDARG00000040135	fosaa	0.022089	1.309648703	47.24462343	117.1105269
ENSDARG00000103720	ZFP36	1.85E-13	1.299530413	2988.236765	7355.507441
ENSDARG00000037618	ddit4	3.42E-09	1.27501897	385.7328554	933.4812243
ENSDARG00000077726	nocta	8.75E-19	1.266065444	605.7805038	1456.930944
ENSDARG00000102916	CABZ01087111.1	0.004947	1.265739382	47.63003889	114.5266235
ENSDARG00000028804	ankrd9	3.50E-09	1.262445692	816.300795	1958.322622
ENSDARG00000061242	tuft1a	1.06E-13	1.249240046	554.990101	1319.301216
ENSDARG00000036028	arrdc3b	2.07E-19	1.241331994	4777.649469	11295.16157
ENSDARG00000059001	pim2	2.86E-08	1.231566539	529.6421755	1243.715453
ENSDARG00000104992	epgn	2.86E-07	1.226206507	293.4571651	686.5460255
ENSDARG00000087844	plekhn1	6.79E-09	1.225008432	182.5294964	426.6751389
ENSDARG00000002509	zgc:153911	0.002727	1.223657533	55.21204324	128.9411209

Table 5.1 (continued).

ENSDARG00000076839	ftr86	0.000361	1.209903926	147.7645487	341.8122518
ENSDARG00000093304	si:dkey-221j11.3	2.61E-05	1.205247379	222.2796625	512.5253396
ENSDARG00000089382	zgc:158463	9.96E-11	1.199133021	41305.66236	94838.48306
ENSDARG00000077169	si:ch211-153b23.4	0.011237	1.194336673	952.7031992	2180.162107
ENSDARG00000009544	cldnb	2.06E-20	1.181573803	1629.343485	3695.743358
ENSDARG00000012390	kcnk5b	2.86E-07	1.17821343	160.2744016	362.6951497
ENSDARG00000098108	dusp2	1.90E-11	1.167923059	305.9080705	687.3387174
ENSDARG00000031426	csrnp1a	4.79E-10	1.153647754	297.1463149	661.0783387
ENSDARG00000031929	stard14	8.87E-16	1.145507658	822.2031293	1818.910335
ENSDARG00000069135	ppp1r15a	1.14E-20	1.137479476	1350.48133	2971.009404
ENSDARG00000030896	foxq1a	0.021734	1.13565406	388.5696718	853.7581005
ENSDARG00000036107	txnipa	9.70E-06	1.132254573	5751.344901	12607.00722
ENSDARG00000043243	prkchb	0.001454	1.130473523	70.16654442	153.6160269
ENSDARG00000039269	arg2	8.83E-08	1.126425617	417.3926321	911.2397939
ENSDARG00000037421	egr1	4.27E-20	1.119914984	2113.145536	4592.587205
ENSDARG00000041294	noxo1a	0.014546	1.094401983	373.2483157	796.9768031
ENSDARG00000027744	gadd45ba	9.76E-08	1.07402027	655.2088936	1379.405969
ENSDARG00000025522	sgk1	2.01E-17	1.065846848	1848.281891	3869.190211
ENSDARG00000020761	arrdc2	1.05E-12	1.060223676	1634.844435	3409.067199
ENSDARG00000076142	trib1	3.72E-08	1.034633036	324.1163849	663.9823953
ENSDARG00000008363	mcl1b	4.37E-08	1.032213387	2219.293815	4538.809906
ENSDARG00000035859	angptl4	1.04E-12	1.022871362	2483.877524	5047.137534
ENSDARG00000015263	adma	4.49E-07	1.015173048	267.9391835	541.544024
ENSDARG00000103162	CABZ01046954.1	0.00154	1.013424321	97.17255607	196.161939

Table 5.1 (continued).

ENSDARG00000079472	F2RL2 (1 of 2)	0.000203	1.009052607	136.0021131	273.7163614
ENSDARG00000055752	npas4a	0.032897	-1.068084043	154.0921166	73.49454166
ENSDARG00000103981	bhlha9	0.000564	-1.078672451	208.9821341	98.94557953
ENSDARG00000102435	plekhf1	1.33E-07	-1.24512015	414.72165	174.9597681
ENSDARG00000091906	rbp7a	0.014728	-1.399870492	77.30410014	29.29540599
ENSDARG00000090526	PLEKHS1 (3 of 3)	5.19E-09	-2.169486316	138.0733401	30.69229578

Table 5.2 Differentially expressed genes: Iso+PA versus Uninjected (log2 fold change>1).

GeneID	GeneSymbol	P.adj	log2[IsoPA/Uninjected]	Mean_counts_Uninjected	Mean_counts_IsoPA
ENSDARG00000098700	il1b	3.03E-10	3.109554085	15.6729073	135.2753349
ENSDARG00000104773	junbb	2.92E-09	1.238102319	767.3552893	1810.099409
ENSDARG00000077169	si:ch211-153b23.4	1.45E-08	1.088653112	965.740329	2053.892028
ENSDARG00000074378	junba	2.30E-07	1.257514102	342.1356262	817.9895655
ENSDARG00000010276	ptgs2b	1.82E-05	1.315881886	355.1377319	884.1312374
ENSDARG00000015355	fosl1a	0.000139	1.189526074	126.4051544	288.3021044
ENSDARG00000076839	ftr86	0.000269	1.282143734	149.809791	364.3375393
ENSDARG00000069377	si:dkey-242g16.2	0.000549	-1.629871024	168.616586	54.48290107
ENSDARG00000041294	noxo1a	0.003032	1.095659362	378.4358035	808.7579279
ENSDARG00000087732	Metazoa_SRP	0.004155	1.284480627	271.6843406	661.8076831
ENSDARG00000019949	serpinh1b	0.014519	-1.413876942	6093.856518	2287.035229
ENSDARG00000076820	xkr8.2	0.016235	-1.565056133	109.4496926	36.99011703

Table 5.3 Summary of experimental numbers.

Experiment type	Experimental groups	Fish treatment	Fish line	# of experimental days	total # of larvae
Ear infection	Uninjected	None	TG(*lysC*:Casper1GR)	2	31
	Hypo PA	None	TG(*lysC*:Casper1GR)	46	330
		cpla$_2$_splicing MO 1	TG(*lysC*:Casper1GR)	6	20
		cpla$_2$_splicing MO 2	TG(*lysC*:Casper1GR)	4	39
		cpla$_2$_ATG MO	TG(*lysC*:Casper1GR)	3	31
		cpla$_2$ wt mRNA	TG(*lysC*:Casper1GR)	3	32
		cpla$_2$ S498A mRNA	TG(*lysC*:Casper1GR)	3	35
		myd88 ATG MO	TG(*lysC*:Casper1GR)	4	27
		myd88 ATG MisPrime	TG(*lysC*:Casper1GR)	4	45
		*pycard*_splicing MO	TG(*lysC*:Casper1GR)	4	16
		DMSO ctrl	TG(*lysC*:Casper1GR)	22	200
		400ug/mL CHX	TG(*lysC*:Casper1GR)	2	23
		100uM Aspirin	TG(*lysC*:Casper1GR)	2	19
		20uM Zileuton	TG(*lysC*:Casper1GR)	3	33
		50uM Licofelone	TG(*lysC*:Casper1GR)	4	36
	Hypo *fleN* PA	None	TG(*lysC*:Casper1GR)	3	26
	Hypo ORF_11 PA	None	TG(*lysC*:Casper1GR)	3	26
	Hypo EGFP PA	None	wt casper	2	6
	Iso EGFP PA	None	wt casper	1	3
	Iso PA	None	TG(*lysC*:Casper1GR)	10	80
		DMSO ctrl	TG(*lysC*:Casper1GR)	3	20
		25 uM AA	TG(*lysC*:Casper1GR)	2	17

Table 5.3 (continued).

Ear infection	Iso *exoU* PA	None	TG(*lysC*:Casper1GR)	8	113
		0.5% Digitonin	TG(*lysC*:Casper1GR)	3	37
		120uM Melittin	TG(*lysC*:Casper1GR)	2	30
	Hypo E3	None	TG(*lysC*:Casper1GR)	17	105
	Iso E3	None	TG(*lysC*:Casper1GR)	6	47
	Hypo *E. coli*	None	TG(*lysC*:Casper1GR)	3	28
	Iso *E. coli*	None	TG(*lysC*:Casper1GR)	3	25
PA survival assay	IsoE3	None	TG(*lysC*:Casper1GR)	4	69
	1/4 Iso PA	None	TG(*lysC*:Casper1GR)	4	66
	1/2 Iso PA	None	TG(*lysC*:Casper1GR)	4	70
	Iso PA	None	TG(*lysC*:Casper1GR)	4	71
	Hypo E3	None	TG(*lysC*:Casper1GR)	4	70
	1/4 Hypo PA	None	TG(*lysC*:Casper1GR)	4	71
	1/2 Hypo PA	None	TG(*lysC*:Casper1GR)	4	69
	Hypo PA	None	TG(*lysC*:Casper1GR)	4	71
Experiment name	Experimental groups	Fish treatment	Fish line	# of experimental days	total # of plates
Muscle infection	Hypo PA	None	TG(*lysC*:Casper1GR)	2	40
	Iso PA	None	TG(*lysC*:Casper1GR)	2	37
Experiment name	Experimental groups	Fish treatment	Fish line	# of experimental days	total # of plates
CFU counting assay	Iso PA	N.A.	N.A	13	39
	Hypo PA	N.A.	N.A	50	164
	Heatkilled PA	N.A.	N.A	1	9
	Iso *exoU* PA	N.A.	N.A.	8	24

Table 5.3 (continued)

CFU counting assay	Iso *exoU* PA 0.5% Digitonin	N.A.	N.A.	3	9
	Iso *exoU* PA 120uM Melittin	N.A.	N.A.	2	6
Experiment name	Experimental groups	Fish treatment	Fish line	total # of larvae	total # of tracks
Trajectory analysis	Uninjected Iso E3	None	TG(*lysC*:Casper1GR)	13	145
	Uninjected Hypo E3	None	TG(*lysC*:Casper1GR)	11	169
	Iso PA	None	TG(*lysC*:Casper1GR)	10	150
	Hypo PA	None	TG(*lysC*:Casper1GR)	12	181
Experiment name	Experimental groups	Fish treatment	Fish line	# of experimental days	total # of larvae
RNA-seq	Uninjected	None	wt casper	3	70
	Iso PA	None	wt casper	3	73
	Hypo PA	None	wt casper	3	66
Experiment name	Experimental groups	Fish treatment	Fish line	# of experimental days	total # of larvae
il1b in situ	Iso E3 (60min)	None	TG(*lysC*:Casper1GR)	1	26
	Hypo E3 (60min)	None	TG(*lysC*:Casper1GR)	1	23
	Iso PA (60min)	None	TG(*lysC*:Casper1GR)	1	22
	Hypo PA (60min)	None	TG(*lysC*:Casper1GR)	2	56
Experiment name	Experimental groups	Fish treatment	Fish line	# of experimental days	total # of larvae
CHX positive ctl	400ug/mL CHX	None	TG(*hsp70*:cPla$_2$-mKate2)	1	2
	DMSO	None	TG(*hsp70*:cPla$_2$-mKate2)	1	3
Experiment name	Experimental groups	Fish treatment	Fish line	# of experimental days	total # of larvae
Ear SYTOX Orange staining	Iso E3	None	wt casper	1	12
	Hypo E3	None	wt casper	1	36

Table 5.3 (continued).

Experiment name	Experimental groups	Fish treatment	Fish line	# of different days	total # of larvae
Detection of $cPla_2$ phosphorylation	Hypo E3	None	TG(*lysC*:Casper1GR)	2	>70
	Hypo PA	None	TG(*lysC*:Casper1GR)	2	>70
Experiment name	Experimental groups	Fish treatment	Fish line	# of experimental days	total # of larvae
western blotting *cpla₂* MO	wt	None	TG(*lysC*:Casper1GR)	1	40
	cpla₂ MO	*cpla₂* MO	TG(*lysC*:Casper1GR)	1	40
Experiment name	Experimental groups	Fish treatment	Fish line	# of experimental days	total # of larvae
RT-PCR *pycard* MO	wt	None	TG(*lysC*:Casper1GR)	3	>30
	pycard MO	*pycard* MO	TG(*lysC*:Casper1GR)	3	>30

Chapter VI: References

Aggad, D., Stein, C., Sieger, D., Mazel, M., Boudinot, P., Herbomel, P., Levraud, J.-P., Lutfalla, G., and Leptin, M. (2010). In vivo analysis of Ifn-γ1 and Ifn-γ2 signaling in zebrafish. J. Immunol. *185*, 6774–6782.

Ajibade, A.A., Wang, H.Y., and Wang, R.-F. (2013). Cell type-specific function of TAK1 in innate immune signaling. Trends Immunol. *34*, 307–316.

Akira, S., and Takeda, K. (2004). Toll-like receptor signalling. Nat. Rev. Immunol. *4*, 499–511.

Alexopoulou, L., Holt, A.C., Medzhitov, R., and Flavell, R.A. (2001). Recognition of double-stranded RNA and activation of NF-kappaB by Toll-like receptor 3. Nature *413*, 732–738.

Aliprantis, A.O., Yang, R.B., Mark, M.R., Suggett, S., Devaux, B., Radolf, J.D., Klimpel, G.R., Godowski, P., and Zychlinsky, A. (1999). Cell activation and apoptosis by bacterial lipoproteins through toll-like receptor-2. Science (80-.). *285*, 736–739.

Altmann, S.M., Mellon, M.T., Distel, D.L., and Kim, C.H. (2003). Molecular and functional analysis of an interferon gene from the zebrafish, Danio rerio. J. Virol. *77*, 1992–2002.

Amatruda, J.F., and Zon, L.I. (1999). Dissecting hematopoiesis and disease using the zebrafish. Dev. Biol. *216*, 1–15.

Amulic, B., Cazalet, C., Hayes, G.L., Metzler, K.D., and Zychlinsky, A. (2012). Neutrophil function: from mechanisms to disease. Annu. Rev. Immunol. *30*, 459–489.

Angosto, D., López-Castejón, G., López-Muñoz, A., Sepulcre, M.P., Arizcun, M., Meseguer, J., and Mulero, V. (2012). Evolution of inflammasome functions in vertebrates: Inflammasome and caspase-1 trigger fish macrophage cell death but are dispensable for the processing of IL-1β. Innate Immun *18*, 815–824.

Arango Duque, G., and Descoteaux, A. (2014). Macrophage cytokines: involvement in immunity and infectious diseases. Front. Immunol. *5*, 491.

Areschoug, T., and Gordon, S. (2008). Pattern recognition receptors and their role in innate immunity: focus on microbial protein ligands. Contrib. Microbiol. *15*, 45–60.

Asea, A., Rehli, M., Kabingu, E., Boch, J.A., Bare, O., Auron, P.E., Stevenson, M.A., and Calderwood, S.K. (2002). Novel signal transduction pathway utilized by extracellular HSP70: role of toll-like receptor (TLR) 2 and TLR4. J. Biol. Chem. *277*, 15028–15034.

Bäckhed, F., Ley, R.E., Sonnenburg, J.L., Peterson, D.A., and Gordon, J.I. (2005). Host-bacterial mutualism in the human intestine. Science (80-.). *307*, 1915–1920.

Barton, G.M., and Medzhitov, R. (2003). Toll-like receptor signaling pathways. Science (80-.). *300*, 1524–1525.

Bertrand, J.Y., Kim, A.D., Violette, E.P., Stachura, D.L., Cisson, J.L., and Traver, D. (2007). Definitive hematopoiesis initiates through a committed erythromyeloid progenitor in the zebrafish embryo. Development *134*, 4147–4156.

Bloes, D.A., Kretschmer, D., and Peschel, A. (2015). Enemy attraction: bacterial agonists for leukocyte chemotaxis receptors. Nat. Rev. Micro. *13*, 95–104.

Bogdan, C., Röllinghoff, M., and Diefenbach, A. (2000). Reactive oxygen and reactive nitrogen intermediates in innate and specific immunity. Curr. Opin. Immunol. *12*, 64–76.

Borregaard, N. (2010). Neutrophils, from marrow to microbes. Immunity *33*, 657–670.

Bulut, Y., Faure, E., Thomas, L., Karahashi, H., Michelsen, K.S., Equils, O., Morrison, S.G., Morrison, R.P., and Arditi, M. (2002). Chlamydial heat shock protein 60 activates macrophages and endothelial cells through Toll-like receptor 4 and MD2 in a MyD88-dependent pathway. J. Immunol. *168*, 1435–1440.

Busso, N., and So, A. (2010). Mechanisms of inflammation in gout. Arthritis Res. Ther. *12*, 206.

Charles A Janeway, J., Travers, P., Walport, M., and Shlomchik, M.J. (2001). Immunobiology - NCBI Bookshelf.

Chen, Z.J. (2012). Ubiquitination in signaling to and activation of IKK. Immunol. Rev. *246*, 95–106.

Chen, G.Y., and Nuñez, G. (2010). Sterile inflammation: sensing and reacting to damage. Nat. Rev. Immunol. *10*, 826–837.

Chen, C.-J., Shi, Y., Hearn, A., Fitzgerald, K., Golenbock, D., Reed, G., Akira, S., and Rock, K.L. (2006). MyD88-dependent IL-1 receptor signaling is essential for gouty inflammation stimulated by monosodium urate crystals. J. Clin. Invest. *116*, 2262–2271.

Cheng, N., He, R., Tian, J., Ye, P.P., and Ye, R.D. (2008). Cutting edge: TLR2 is a functional receptor for acute-phase serum amyloid A. J. Immunol. *181*, 22–26.

Chow, J.C., Young, D.W., Golenbock, D.T., Christ, W.J., and Gusovsky, F. (1999). Toll-like receptor-4 mediates lipopolysaccharide-induced signal transduction. J. Biol. Chem. *274*, 10689–10692.

Clatworthy, A.E., Lee, J.S.-W., Leibman, M., Kostun, Z., Davidson, A.J., and Hung, D.T. (2009). Pseudomonas aeruginosa infection of zebrafish involves both host and pathogen determinants. Infect. Immun. *77*, 1293–1303.

Clay, H., Volkman, H.E., and Ramakrishnan, L. (2008). Tumor necrosis factor signaling mediates resistance to mycobacteria by inhibiting bacterial growth and macrophage death. Immunity *29*, 283–294.

Compan, V., Baroja-Mazo, A., López-Castejón, G., Gomez, A.I., Martínez, C.M., Angosto, D., Montero, M.T., Herranz, A.S., Bazán, E., Reimers, D., et al. (2012). Cell volume regulation modulates NLRP3 inflammasome activation. Immunity *37*, 487–500.

Coussens, L.M., and Werb, Z. (2002). Inflammation and cancer. Nature *420*, 860–867.

Curran, C.S., Demick, K.P., and Mansfield, J.M. (2006). Lactoferrin activates macrophages via TLR4-dependent and -independent signaling pathways. Cell Immunol. *242*, 23–30.

Dacheux, D., Goure, J., Chabert, J., Usson, Y., and Attree, I. (2001). Pore-forming activity of type III system-secreted proteins leads to oncosis of Pseudomonas aeruginosa-infected macrophages. Mol. Microbiol. *40*, 76–85.

Davis, J.M., and Ramakrishnan, L. (2009). The role of the granuloma in expansion and dissemination of early tuberculous infection. Cell *136*, 37–49.

Davis, J.M., Clay, H., Lewis, J.L., Ghori, N., Herbomel, P., and Ramakrishnan, L. (2002). Real-time visualization of mycobacterium-macrophage interactions leading to initiation of granuloma formation in zebrafish embryos. Immunity *17*, 693–702.

Deng, Q., Harvie, E.A., and Huttenlocher, A. (2012). Distinct signalling mechanisms mediate neutrophil attraction to bacterial infection and tissue injury. Cell Microbiol. *14*, 517–528.

Dennis, E.A., and Norris, P.C. (2015). Eicosanoid storm in infection and inflammation. Nat. Rev. Immunol. *15*, 511–523.

Dennis, E.A., Cao, J., Hsu, Y.-H., Magrioti, V., and Kokotos, G. (2011). Phospholipase A2 enzymes: physical structure, biological function, disease implication, chemical inhibition, and therapeutic intervention. Chem. Rev. *111*, 6130–6185.

Devaney, J.M., Greene, C.M., Taggart, C.C., Carroll, T.P., O'Neill, S.J., and McElvaney, N.G. (2003). Neutrophil elastase up-regulates interleukin-8 via toll-like receptor 4. FEBS Lett. *544*, 129–132.

Dobin, A., Davis, C.A., Schlesinger, F., Drenkow, J., Zaleski, C., Jha, S., Batut, P., Chaisson, M., and Gingeras, T.R. (2013). STAR: ultrafast universal RNA-seq aligner. Bioinformatics *29*, 15–21.

Dooley, K., and Zon, L.I. (2000). Zebrafish: a model system for the study of human disease. Curr. Opin. Genet. Dev. *10*, 252–256.

Dovi, J.V., He, L.-K., and DiPietro, L.A. (2003). Accelerated wound closure in neutrophil-depleted mice. J. Leukoc. Biol. *73*, 448–455.

Dovi, J.V., Szpaderska, A.M., and DiPietro, L.A. (2004). Neutrophil function in the healing wound: adding insult to injury? Thromb. Haemost. *92*, 275–280.

Driever, W., Solnica-Krezel, L., Schier, A.F., Neuhauss, S.C., Malicki, J., Stemple, D.L., Stainier, D.Y., Zwartkruis, F., Abdelilah, S., Rangini, Z., et al. (1996). A genetic screen for mutations affecting embryogenesis in zebrafish. Development *123*, 37–46.

Eliopoulos, A.G., Dumitru, C.D., Wang, C.-C., Cho, J., and Tsichlis, P.N. (2002). Induction of COX-2 by LPS in macrophages is regulated by Tpl2-dependent CREB activation signals. EMBO J. *21*, 4831–4840.

Ellett, F., Pase, L., Hayman, J.W., Andrianopoulos, A., and Lieschke, G.J. (2011). mpeg1 promoter transgenes direct macrophage-lineage expression in zebrafish. Blood *117*, e49–56.

Engström, P.G., Steijger, T., Sipos, B., Grant, G.R., Kahles, A., Rätsch, G., Goldman, N., Hubbard, T.J., Harrow, J., Guigó, R., et al. (2013). Systematic evaluation of spliced alignment programs for RNA-seq data. Nat. Methods *10*, 1185–1191.

Enyedi, B., and Niethammer, P. (2017). Nuclear membrane stretch and its role in mechanotransduction. Nucleus *8*, 156–161.

Enyedi, B., Kala, S., Nikolich-Zugich, T., and Niethammer, P. (2013). Tissue damage detection by osmotic surveillance. Nat. Cell Biol. *15*, 1123–1130.

Enyedi, B., Jelcic, M., and Niethammer, P. (2016). The Cell Nucleus Serves as a Mechanotransducer of Tissue Damage-Induced Inflammation. Cell *165*, 1160–1170.

Feinbaum, R.L., Urbach, J.M., Liberati, N.T., Djonovic, S., Adonizio, A., Carvunis, A.-R., and Ausubel, F.M. (2012). Genome-wide identification of Pseudomonas aeruginosa virulence-related genes using a Caenorhabditis elegans infection model. PLoS Pathog. *8*, e1002813.

Feng, Y., and Martin, P. (2015). Imaging innate immune responses at tumour initiation: new insights from fish and flies. Nat. Rev. Cancer *15*, 556–562.

Finck-Barbançon, V., Goranson, J., Zhu, L., Sawa, T., Wiener-Kronish, J.P., Fleiszig, S.M., Wu, C., Mende-Mueller, L., and Frank, D.W. (1997). ExoU expression by Pseudomonas aeruginosa correlates with acute cytotoxicity and epithelial injury. Mol. Microbiol. *25*, 547–557.

Fitsialos, G., Chassot, A.-A., Turchi, L., Dayem, M.A., LeBrigand, K., Moreilhon, C., Meneguzzi, G., Buscà, R., Mari, B., Barbry, P., et al. (2007). Transcriptional signature of epidermal keratinocytes subjected to in vitro scratch wounding reveals

selective roles for ERK1/2, p38, and phosphatidylinositol 3-kinase signaling pathways. J. Biol. Chem. *282*, 15090–15102.

Fitzpatrick, F.A., and Soberman, R. (2001). Regulated formation of eicosanoids. J. Clin. Invest. *107*, 1347–1351.

Flores, M.V., Crawford, K.C., Pullin, L.M., Hall, C.J., Crosier, K.E., and Crosier, P.S. (2010). Dual oxidase in the intestinal epithelium of zebrafish larvae has anti-bacterial properties. Biochem. Biophys. Res. Commun. *400*, 164–168.

Flynn, J.L. (2006). Lessons from experimental Mycobacterium tuberculosis infections. Microbes Infect. *8*, 1179–1188.

Foell, D., Wittkowski, H., Vogl, T., and Roth, J. (2007). S100 proteins expressed in phagocytes: a novel group of damage-associated molecular pattern molecules. J. Leukoc. Biol. *81*, 28–37.

Forn-Cuní, G., Varela, M., Pereiro, P., Novoa, B., and Figueras, A. (2017). Conserved gene regulation during acute inflammation between zebrafish and mammals. Sci. Rep. *7*, 41905.

Franchi, L., Park, J.-H., Shaw, M.H., Marina-Garcia, N., Chen, G., Kim, Y.-G., and Núñez, G. (2008). Intracellular NOD-like receptors in innate immunity, infection and disease. Cell Microbiol. *10*, 1–8.

Funderburg, N., Lederman, M.M., Feng, Z., Drage, M.G., Jadlowsky, J., Harding, C.V., Weinberg, A., and Sieg, S.F. (2007). Human -defensin-3 activates professional antigen-presenting cells via Toll-like receptors 1 and 2. Proc. Natl. Acad. Sci. USA *104*, 18631–18635.

Gault, W.J., Enyedi, B., and Niethammer, P. (2014). Osmotic surveillance mediates rapid wound closure through nucleotide release. J. Cell Biol. *207*, 767–782.

Geddes, K., Magalhães, J.G., and Girardin, S.E. (2009). Unleashing the therapeutic potential of NOD-like receptors. Nat. Rev. Drug Discov. *8*, 465–479.

Gerlach, G.F., and Wingert, R.A. (2014). Zebrafish pronephros tubulogenesis and epithelial identity maintenance are reliant on the polarity proteins Prkc iota and zeta. Dev. Biol. *396*, 183–200.

Gordon, S. (2003). Alternative activation of macrophages. Nat. Rev. Immunol. *3*, 23–35.

Gross, O., Thomas, C.J., Guarda, G., and Tschopp, J. (2011). The inflammasome: an integrated view. Immunol. Rev. *243*, 136–151.

Hadgraft, J. (2001). Skin, the final frontier. Int. J. Pharm. *224*, 1–18.

Haffter, P., Granato, M., Brand, M., Mullins, M.C., Hammerschmidt, M., Kane, D.A., Odenthal, J., van Eeden, F.J., Jiang, Y.J., Heisenberg, C.P., et al. (1996). The

identification of genes with unique and essential functions in the development of the zebrafish, Danio rerio. Development *123*, 1–36.

Hall, C., Flores, M.V., Storm, T., Crosier, K., and Crosier, P. (2007). The zebrafish lysozyme C promoter drives myeloid-specific expression in transgenic fish. BMC Dev. Biol. *7*, 42.

Harvie, E.A., and Huttenlocher, A. (2015). Neutrophils in host defense: new insights from zebrafish. J. Leukoc. Biol. *98*, 523–537.

Hauser, A.R., and Engel, J.N. (1999). Pseudomonas aeruginosa induces type-III-secretion-mediated apoptosis of macrophages and epithelial cells. Infect. Immun. *67*, 5530–5537.

Hayashi, F., Smith, K.D., Ozinsky, A., Hawn, T.R., Yi, E.C., Goodlett, D.R., Eng, J.K., Akira, S., Underhill, D.M., and Aderem, A. (2001). The innate immune response to bacterial flagellin is mediated by Toll-like receptor 5. Nature *410*, 1099–1103.

He, R.L., Zhou, J., Hanson, C.Z., Chen, J., Cheng, N., and Ye, R.D. (2009). Serum amyloid A induces G-CSF expression and neutrophilia via Toll-like receptor 2. Blood *113*, 429–437.

Heil, F., Hemmi, H., Hochrein, H., Ampenberger, F., Kirschning, C., Akira, S., Lipford, G., Wagner, H., and Bauer, S. (2004). Species-specific recognition of single-stranded RNA via toll-like receptor 7 and 8. Science (80-.). *303*, 1526–1529.

Heilmann, S., Ratnakumar, K., Langdon, E., Kansler, E., Kim, I., Campbell, N.R., Perry, E., McMahon, A., Kaufman, C., van Rooijen, E., et al. (2015). A quantitative system for studying metastasis using transparent zebrafish. Cancer Res. *75*, 4272–4282.

Helander, H.F., and Fändriks, L. (2014). Surface area of the digestive tract - revisited. Scand. J. Gastroenterol. *49*, 681–689.

Hemmi, H., Takeuchi, O., Kawai, T., Kaisho, T., Sato, S., Sanjo, H., Matsumoto, M., Hoshino, K., Wagner, H., Takeda, K., et al. (2000). A Toll-like receptor recognizes bacterial DNA. Nature *408*, 740–745.

Herbomel, P., Thisse, B., and Thisse, C. (1999). Ontogeny and behaviour of early macrophages in the zebrafish embryo. Development *126*, 3735–3745.

Hiratsuka, S., Watanabe, A., Sakurai, Y., Akashi-Takamura, S., Ishibashi, S., Miyake, K., Shibuya, M., Akira, S., Aburatani, H., and Maru, Y. (2008). The S100A8-serum amyloid A3-TLR4 paracrine cascade establishes a pre-metastatic phase. Nat. Cell Biol. *10*, 1349–1355.

Hirschfeld, M., Weis, J.J., Toshchakov, V., Salkowski, C.A., Cody, M.J., Ward, D.C., Qureshi, N., Michalek, S.M., and Vogel, S.N. (2001). Signaling by toll-like receptor 2

and 4 agonists results in differential gene expression in murine macrophages. Infect. Immun. *69*, 1477–1482.

Hisaoka, K.K., and Firlit, C.F. (1962). Ovarian Cycle and Egg Production in the Zebrafish, Brachydanio rerio. Copeia *1962*, 788.

Howe, K., Clark, M.D., Torroja, C.F., Torrance, J., Berthelot, C., Muffato, M., Collins, J.E., Humphray, S., McLaren, K., Matthews, L., et al. (2013). The zebrafish reference genome sequence and its relationship to the human genome. Nature *496*, 498–503.

Howe, K., Schiffer, P.H., Zielinski, J., Wiehe, T., Laird, G.K., Marioni, J.C., Soylemez, O., Kondrashov, F., and Leptin, M. (2016). Structure and evolutionary history of a large family of NLR proteins in the zebrafish. Open Biol *6*, 160009.

Hruscha, A., Krawitz, P., Rechenberg, A., Heinrich, V., Hecht, J., Haass, C., and Schmid, B. (2013). Efficient CRISPR/Cas9 genome editing with low off-target effects in zebrafish. Development *140*, 4982–4987.

Huising, M.O., Stet, R.J.M., Savelkoul, H.F.J., and Verburg-van Kemenade, B.M.L. (2004). The molecular evolution of the interleukin-1 family of cytokines; IL-18 in teleost fish. Dev. Comp. Immunol. *28*, 395–413.

Hurley, B.P., Williams, N.L., and McCormick, B.A. (2006). Involvement of phospholipase A2 in Pseudomonas aeruginosa-mediated PMN transepithelial migration. Am. J. Physiol. Lung Cell Mol. Physiol. *290*, L703–L709.

Hurley, B.P., Pirzai, W., Mumy, K.L., Gronert, K., and McCormick, B.A. (2011). Selective eicosanoid-generating capacity of cytoplasmic phospholipase A2 in Pseudomonas aeruginosa-infected epithelial cells. Am. J. Physiol. Lung Cell Mol. Physiol. *300*, L286–94.

Hurst, J., Prinz, N., Lorenz, M., Bauer, S., Chapman, J., Lackner, K.J., and von Landenberg, P. (2009). TLR7 and TLR8 ligands and antiphospholipid antibodies show synergistic effects on the induction of IL-1beta and caspase-1 in monocytes and dendritic cells. Immunobiology *214*, 683–691.

Ignatius, M.S., Hayes, M., and Langenau, D.M. (2016). In Vivo Imaging of Cancer in Zebrafish. Adv. Exp. Med. Biol. *916*, 219–237.

Jao, L.-E., Wente, S.R., and Chen, W. (2013). Efficient multiplex biallelic zebrafish genome editing using a CRISPR nuclease system. Proc. Natl. Acad. Sci. USA *110*, 13904–13909.

De Jong, J.L.O., and Zon, L.I. (2005). Use of the zebrafish system to study primitive and definitive hematopoiesis. Annu. Rev. Genet. *39*, 481–501.

Kalogeris, T., Baines, C.P., Krenz, M., and Korthuis, R.J. (2012). Cell biology of ischemia/reperfusion injury. Int. Rev. Cell Mol. Biol. *298*, 229–317.

Kanneganti, T.-D., Body-Malapel, M., Amer, A., Park, J.-H., Whitfield, J., Franchi, L., Taraporewala, Z.F., Miller, D., Patton, J.T., Inohara, N., et al. (2006). Critical role for Cryopyrin/Nalp3 in activation of caspase-1 in response to viral infection and double-stranded RNA. J. Biol. Chem. *281*, 36560–36568.

Kawahara, T., Kohjima, M., Kuwano, Y., Mino, H., Teshima-Kondo, S., Takeya, R., Tsunawaki, S., Wada, A., Sumimoto, H., and Rokutan, K. (2005). Helicobacter pylori lipopolysaccharide activates Rac1 and transcription of NADPH oxidase Nox1 and its organizer NOXO1 in guinea pig gastric mucosal cells. Am. J. Physiol. Cell Physiol. *288*, C450–7.

Kawai, T., and Akira, S. (2007). TLR signaling. Semin. Immunol. *19*, 24–32.

Kawasaki, T., and Kawai, T. (2014). Toll-like receptor signaling pathways. Front. Immunol. *5*, 461.

Kayagaki, N., Wong, M.T., Stowe, I.B., Ramani, S.R., Gonzalez, L.C., Akashi-Takamura, S., Miyake, K., Zhang, J., Lee, W.P., Muszyński, A., et al. (2013). Noncanonical inflammasome activation by intracellular LPS independent of TLR4. Science (80-.). *341*, 1246–1249.

Kimmel, C.B., Ballard, W.W., Kimmel, S.R., Ullmann, B., and Schilling, T.F. (1995). Stages of embryonic development of the zebrafish. Dev. Dyn. *203*, 253–310.

Koh, T.J., and DiPietro, L.A. (2011). Inflammation and wound healing: the role of the macrophage. Expert Rev Mol Med *13*, e23.

Kokkola, R., Andersson, A., Mullins, G., Ostberg, T., Treutiger, C.J., Arnold, B., Nawroth, P., Andersson, U., Harris, R.A., and Harris, H.E. (2005). RAGE is the major receptor for the proinflammatory activity of HMGB1 in rodent macrophages. Scand. J. Immunol. *61*, 1–9.

Kollewe, C., Mackensen, A.-C., Neumann, D., Knop, J., Cao, P., Li, S., Wesche, H., and Martin, M.U. (2004). Sequential autophosphorylation steps in the interleukin-1 receptor-associated kinase-1 regulate its availability as an adapter in interleukin-1 signaling. J. Biol. Chem. *279*, 5227–5236.

Kono, H., and Rock, K.L. (2008). How dying cells alert the immune system to danger. Nat. Rev. Immunol. *8*, 279–289.

Kurt-Jones, E.A., Popova, L., Kwinn, L., Haynes, L.M., Jones, L.P., Tripp, R.A., Walsh, E.E., Freeman, M.W., Golenbock, D.T., Anderson, L.J., et al. (2000). Pattern recognition receptors TLR4 and CD14 mediate response to respiratory syncytial virus. Nat. Immunol. *1*, 398–401.

Kwan, K.M., Fujimoto, E., Grabher, C., Mangum, B.D., Hardy, M.E., Campbell, D.S., Parant, J.M., Yost, H.J., Kanki, J.P., and Chien, C.-B. (2007). The Tol2kit: a multisite

gateway-based construction kit for Tol2 transposon transgenesis constructs. Dev. Dyn. *236*, 3088–3099.

Kyritsis, N., Kizil, C., Zocher, S., Kroehne, V., Kaslin, J., Freudenreich, D., Iltzsche, A., and Brand, M. (2012). Acute inflammation initiates the regenerative response in the adult zebrafish brain. Science (80-.). *338*, 1353–1356.

Lacy, P. (2006). Mechanisms of degranulation in neutrophils. Allergy Asthma. Clin. Immunol. *2*, 98–108.

Laing, K.J., Purcell, M.K., Winton, J.R., and Hansen, J.D. (2008). A genomic view of the NOD-like receptor family in teleost fish: identification of a novel NLR subfamily in zebrafish. BMC Evol. Biol. *8*, 42.

Lämmermann, T., Afonso, P.V., Angermann, B.R., Wang, J.M., Kastenmüller, W., Parent, C.A., and Germain, R.N. (2013). Neutrophil swarms require LTB4 and integrins at sites of cell death in vivo. Nature *498*, 371–375.

Lamprecht, M.R., Sabatini, D.M., and Carpenter, A.E. (2007). CellProfiler: free, versatile software for automated biological image analysis. BioTechniques *42*, 71–75.

Lawrence, T., Willoughby, D.A., and Gilroy, D.W. (2002). Anti-inflammatory lipid mediators and insights into the resolution of inflammation. Nat. Rev. Immunol. *2*, 787–795.

Leadbetter, E.A., Rifkin, I.R., Hohlbaum, A.M., Beaudette, B.C., Shlomchik, M.J., and Marshak-Rothstein, A. (2002). Chromatin-IgG complexes activate B cells by dual engagement of IgM and Toll-like receptors. Nature *416*, 603–607.

Ley, K. (2003). The role of selectins in inflammation and disease. Trends Mol. Med. *9*, 263–268.

Ley, K., Laudanna, C., Cybulsky, M.I., and Nourshargh, S. (2007). Getting to the site of inflammation: the leukocyte adhesion cascade updated. Nat. Rev. Immunol. *7*, 678–689.

Liang, D., Bhatta, S., Gerzanich, V., and Simard, J.M. (2007). Cytotoxic edema: mechanisms of pathological cell swelling. Neurosurg. Focus *22*, E2.

Lieschke, G.J., and Currie, P.D. (2007). Animal models of human disease: zebrafish swim into view. Nat. Rev. Genet. *8*, 353–367.

Lindner, S.C., Köhl, U., Maier, T.J., Steinhilber, D., and Sorg, B.L. (2009). TLR2 ligands augment cPLA2alpha activity and lead to enhanced leukotriene release in human monocytes. J. Leukoc. Biol. *86*, 389–399.

Liu, T., Yamaguchi, Y., Shirasaki, Y., Shikada, K., Yamagishi, M., Hoshino, K., Kaisho, T., Takemoto, K., Suzuki, T., Kuranaga, E., et al. (2014). Single-cell imaging

of caspase-1 dynamics reveals an all-or-none inflammasome signaling response. Cell Rep. *8*, 974–982.

López-Muñoz, A., Roca, F.J., Meseguer, J., and Mulero, V. (2009). New insights into the evolution of IFNs: zebrafish group II IFNs induce a rapid and transient expression of IFN-dependent genes and display powerful antiviral activities. J. Immunol. *182*, 3440–3449.

López-Muñoz, A., Sepulcre, M.P., Roca, F.J., Figueras, A., Meseguer, J., and Mulero, V. (2011). Evolutionary conserved pro-inflammatory and antigen presentation functions of zebrafish IFNγ revealed by transcriptomic and functional analysis. Mol. Immunol. *48*, 1073–1083.

Mahdavian Delavary, B., van der Veer, W.M., van Egmond, M., Niessen, F.B., and Beelen, R.H.J. (2011). Macrophages in skin injury and repair. Immunobiology *216*, 753–762.

Majno, G., and Joris, I. (1995). Apoptosis, oncosis, and necrosis. An overview of cell death. Am. J. Pathol. *146*, 3–15.

Mancuso, G., Gambuzza, M., Midiri, A., Biondo, C., Papasergi, S., Akira, S., Teti, G., and Beninati, C. (2009). Bacterial recognition by TLR7 in the lysosomes of conventional dendritic cells. Nat. Immunol. *10*, 587–594.

Mariathasan, S., Newton, K., Monack, D.M., Vucic, D., French, D.M., Lee, W.P., Roose-Girma, M., Erickson, S., and Dixit, V.M. (2004). Differential activation of the inflammasome by caspase-1 adaptors ASC and Ipaf. Nature *430*, 213–218.

Mariathasan, S., Weiss, D.S., Newton, K., McBride, J., O'Rourke, K., Roose-Girma, M., Lee, W.P., Weinrauch, Y., Monack, D.M., and Dixit, V.M. (2006). Cryopyrin activates the inflammasome in response to toxins and ATP. Nature *440*, 228–232.

Martinon, F., Agostini, L., Meylan, E., and Tschopp, J. (2004). Identification of bacterial muramyl dipeptide as activator of the NALP3/cryopyrin inflammasome. Curr. Biol. *14*, 1929–1934.

Martinon, F., Pétrilli, V., Mayor, A., Tardivel, A., and Tschopp, J. (2006). Gout-associated uric acid crystals activate the NALP3 inflammasome. Nature *440*, 237–241.

Massari, P., Henneke, P., Ho, Y., Latz, E., Golenbock, D.T., and Wetzler, L.M. (2002). Cutting edge: Immune stimulation by neisserial porins is toll-like receptor 2 and MyD88 dependent. J. Immunol. *168*, 1533–1537.

Masud, S., Torraca, V., and Meijer, A.H. (2017). Modeling infectious diseases in the context of a developing immune system. Curr Top Dev Biol *124*, 277–329.

Mathias, J.R., Dodd, M.E., Walters, K.B., Yoo, S.K., Ranheim, E.A., and Huttenlocher, A. (2009). Characterization of zebrafish larval inflammatory macrophages. Dev. Comp. Immunol. *33*, 1212–1217.

Matsumoto, T., Tateda, K., Miyazaki, S., Furuya, N., Ohno, A., Ishii, Y., Hirakata, Y., and Yamaguchi, K. (1998). Effect of immunisation with Pseudomonas aeruginosa on gut-derived sepsis in mice. J. Med. Microbiol. *47*, 295–301.

Matsuo, A., Oshiumi, H., Tsujita, T., Mitani, H., Kasai, H., Yoshimizu, M., Matsumoto, M., and Seya, T. (2008). Teleost TLR22 recognizes RNA duplex to induce IFN and protect cells from birnaviruses. J. Immunol. *181*, 3474–3485.

Matzinger, P. (2002). The danger model: a renewed sense of self. Science (80-.). *296*, 301–305.

Mayadas, T.N., Cullere, X., and Lowell, C.A. (2014). The multifaceted functions of neutrophils. Annu. Rev. Pathol. *9*, 181–218.

McDonald, B., Pittman, K., Menezes, G.B., Hirota, S.A., Slaba, I., Waterhouse, C.C.M., Beck, P.L., Muruve, D.A., and Kubes, P. (2010). Intravascular danger signals guide neutrophils to sites of sterile inflammation. Science (80-.). *330*, 362–366.

McEver, R.P., and Cummings, R.D. (1997). Role of PSGL-1 binding to selectins in leukocyte recruitment. J. Clin. Invest. *100*, S97–103.

McLachlan, G., and Peel, D. (2000). Finite Mixture Models (Hoboken, NJ, USA: John Wiley & Sons, Inc.).

Medzhitov, R. (2008). Origin and physiological roles of inflammation. Nature *454*, 428–435.

Meijer, A.H. (2016). Protection and pathology in TB: learning from the zebrafish model. Semin Immunopathol *38*, 261–273.

Meijering, E., Dzyubachyk, O., and Smal, I. (2012). Methods for cell and particle tracking. Meth. Enzymol. *504*, 183–200.

Mogensen, T.H. (2009). Pathogen recognition and inflammatory signaling in innate immune defenses. Clin. Microbiol. Rev. *22*, 240–73, Table of Contents.

Mosser, D.M. (2003). The many faces of macrophage activation. J. Leukoc. Biol. *73*, 209–212.

Mulla, M.J., Brosens, J.J., Chamley, L.W., Giles, I., Pericleous, C., Rahman, A., Joyce, S.K., Panda, B., Paidas, M.J., and Abrahams, V.M. (2009). Antiphospholipid antibodies induce a pro-inflammatory response in first trimester trophoblast via the TLR4/MyD88 pathway. Am J Reprod Immunol *62*, 96–111.

Muñoz-Planillo, R., Kuffa, P., Martínez-Colón, G., Smith, B.L., Rajendiran, T.M., and Núñez, G. (2013). K^+ efflux is the common trigger of NLRP3 inflammasome activation by bacterial toxins and particulate matter. Immunity *38*, 1142–1153.

Muruve, D.A., Pétrilli, V., Zaiss, A.K., White, L.R., Clark, S.A., Ross, P.J., Parks, R.J., and Tschopp, J. (2008). The inflammasome recognizes cytosolic microbial and host DNA and triggers an innate immune response. Nature *452*, 103–107.

Nasevicius, A., and Ekker, S.C. (2000). Effective targeted gene "knockdown" in zebrafish. Nat. Genet. *26*, 216–220.

Nathan, C. (2002). Points of control in inflammation. Nature *420*, 846–852.

Nathan, C. (2006). Neutrophils and immunity: challenges and opportunities. Nat. Rev. Immunol. *6*, 173–182.

Netea, M.G., Simon, A., van de Veerdonk, F., Kullberg, B.-J., Van der Meer, J.W.M., and Joosten, L.A.B. (2010). IL-1beta processing in host defense: beyond the inflammasomes. PLoS Pathog. *6*, e1000661.

Newton, K., and Dixit, V.M. (2012). Signaling in innate immunity and inflammation. Cold Spring Harb. Perspect. Biol. *4*.

Ng, L.G., Qin, J.S., Roediger, B., Wang, Y., Jain, R., Cavanagh, L.L., Smith, A.L., Jones, C.A., de Veer, M., Grimbaldeston, M.A., et al. (2011). Visualizing the neutrophil response to sterile tissue injury in mouse dermis reveals a three-phase cascade of events. J. Invest. Dermatol. *131*, 2058–2068.

Niess, J.H., and Reinecker, H.-C. (2006). Dendritic cells in the recognition of intestinal microbiota. Cell Microbiol. *8*, 558–564.

Niethammer, P. (2016). The early wound signals. Curr. Opin. Genet. Dev. *40*, 17–22.

Niethammer, P., Grabher, C., Look, A.T., and Mitchison, T.J. (2009). A tissue-scale gradient of hydrogen peroxide mediates rapid wound detection in zebrafish. Nature *459*, 996–999.

Novoa, B., and Figueras, A. (2012). Zebrafish: model for the study of inflammation and the innate immune response to infectious diseases. Adv. Exp. Med. Biol. *946*, 253–275.

Nüsslein-Volhard, C. (Christiane), and Dahm, R. Zebrafish: A practical approach (Oxford: Oxford University Press).

Nuzzi, P.A., Lokuta, M.A., and Huttenlocher, A. (2007). Analysis of neutrophil chemotaxis. Methods Mol. Biol. *370*, 23–36.

Oehlers, S.H., Flores, M.V., Hall, C.J., Swift, S., Crosier, K.E., and Crosier, P.S. (2011). The inflammatory bowel disease (IBD) susceptibility genes NOD1 and NOD2 have conserved anti-bacterial roles in zebrafish. Dis. Model. Mech. *4*, 832–841.

Ohashi, K., Burkart, V., Flohé, S., and Kolb, H. (2000). Cutting edge: heat shock protein 60 is a putative endogenous ligand of the toll-like receptor-4 complex. J. Immunol. *164*, 558–561.

Ordas, A., Hegedus, Z., Henkel, C.V., Stockhammer, O.W., Butler, D., Jansen, H.J., Racz, P., Mink, M., Spaink, H.P., and Meijer, A.H. (2011). Deep sequencing of the innate immune transcriptomic response of zebrafish embryos to Salmonella infection. Fish Shellfish Immunol. *31*, 716–724.

Palha, N., Guivel-Benhassine, F., Briolat, V., Lutfalla, G., Sourisseau, M., Ellett, F., Wang, C.-H., Lieschke, G.J., Herbomel, P., Schwartz, O., et al. (2013). Real-time whole-body visualization of Chikungunya Virus infection and host interferon response in zebrafish. PLoS Pathog. *9*, e1003619.

Park, B.S., and Lee, J.-O. (2013). Recognition of lipopolysaccharide pattern by TLR4 complexes. Exp Mol Med *45*, e66.

Park, J.-H., Kim, Y.-G., McDonald, C., Kanneganti, T.-D., Hasegawa, M., Body-Malapel, M., Inohara, N., and Núñez, G. (2007). RICK/RIP2 mediates innate immune responses induced through Nod1 and Nod2 but not TLRs. J. Immunol. *178*, 2380–2386.

Park, J.S., Svetkauskaite, D., He, Q., Kim, J.-Y., Strassheim, D., Ishizaka, A., and Abraham, E. (2004). Involvement of toll-like receptors 2 and 4 in cellular activation by high mobility group box 1 protein. J. Biol. Chem. *279*, 7370–7377.

Park, J.S., Gamboni-Robertson, F., He, Q., Svetkauskaite, D., Kim, J.-Y., Strassheim, D., Sohn, J.-W., Yamada, S., Maruyama, I., Banerjee, A., et al. (2006). High mobility group box 1 protein interacts with multiple Toll-like receptors. Am. J. Physiol. Cell Physiol. *290*, C917–24.

Patton, E.E., and Zon, L.I. (2001). The art and design of genetic screens: zebrafish. Nat. Rev. Genet. *2*, 956–966.

Pétrilli, V., Papin, S., Dostert, C., Mayor, A., Martinon, F., and Tschopp, J. (2007). Activation of the NALP3 inflammasome is triggered by low intracellular potassium concentration. Cell Death Differ. *14*, 1583–1589.

Piccinini, A.M., and Midwood, K.S. (2010). DAMPening inflammation by modulating TLR signalling. Mediators Inflamm. *2010*.

Picoli, T., Peter, C.M., Zani, J.L., Waller, S.B., Lopes, M.G., Boesche, K.N., Vargas, G.D.Á., Hübner, S. de O., and Fischer, G. (2017). Melittin and its potential in the destruction and inhibition of the biofilm formation by Staphylococcus aureus, Escherichia coli and Pseudomonas aeruginosa isolated from bovine milk. Microb. Pathog. *112*, 57–62.

Poltorak, A., He, X., Smirnova, I., Liu, M.Y., Van Huffel, C., Du, X., Birdwell, D., Alejos, E., Silva, M., Galanos, C., et al. (1998). Defective LPS signaling in C3H/HeJ and C57BL/10ScCr mice: mutations in Tlr4 gene. Science (80-.). *282*, 2085–2088.

Progatzky, F., Sangha, N.J., Yoshida, N., McBrien, M., Cheung, J., Shia, A., Scott, J., Marchesi, J.R., Lamb, J.R., Bugeon, L., et al. (2014). Dietary cholesterol directly induces acute inflammasome-dependent intestinal inflammation. Nat Commun *5*, 5864.

Purcell, M.K., Smith, K.D., Hood, L., Winton, J.R., and Roach, J.C. (2006). Conservation of Toll-Like Receptor Signaling Pathways in Teleost Fish. Comp. Biochem. Physiol. Part D. Genomics Proteomics.

Qi, H.-Y., and Shelhamer, J.H. (2005). Toll-like receptor 4 signaling regulates cytosolic phospholipase A2 activation and lipid generation in lipopolysaccharide-stimulated macrophages. J. Biol. Chem. *280*, 38969–38975.

Rådmark, O., Werz, O., Steinhilber, D., and Samuelsson, B. (2015). 5-Lipoxygenase, a key enzyme for leukotriene biosynthesis in health and disease. Biochim. Biophys. Acta *1851*, 331–339.

Ramakrishnan, L. (2012). Revisiting the role of the granuloma in tuberculosis. Nat. Rev. Immunol. *12*, 352–366.

Ramakrishnan, L. (2013a). The zebrafish guide to tuberculosis immunity and treatment. Cold Spring Harb. Symp. Quant. Biol. *78*, 179–192.

Ramakrishnan, L. (2013b). Looking within the zebrafish to understand the tuberculous granuloma. Adv. Exp. Med. Biol. *783*, 251–266.

Rassa, J.C., Meyers, J.L., Zhang, Y., Kudaravalli, R., and Ross, S.R. (2002). Murine retroviruses activate B cells via interaction with toll-like receptor 4. Proc. Natl. Acad. Sci. USA *99*, 2281–2286.

Redd, M.J., Kelly, G., Dunn, G., Way, M., and Martin, P. (2006). Imaging macrophage chemotaxis in vivo: studies of microtubule function in zebrafish wound inflammation. Cell Motil. Cytoskeleton *63*, 415–422.

Renshaw, S.A., Loynes, C.A., Trushell, D.M.I., Elworthy, S., Ingham, P.W., and Whyte, M.K.B. (2006). A transgenic zebrafish model of neutrophilic inflammation. Blood *108*, 3976–3978.

Renshaw, S.A., Loynes, C.A., Elworthy, S., Ingham, P.W., and Whyte, M.K.B. (2007). Modeling inflammation in the zebrafish: how a fish can help us understand lung disease. Exp Lung Res *33*, 549–554.

Ribeiro, C.M.S., Hermsen, T., Taverne-Thiele, A.J., Savelkoul, H.F.J., and Wiegertjes, G.F. (2010). Evolution of recognition of ligands from Gram-positive

bacteria: similarities and differences in the TLR2-mediated response between mammalian vertebrates and teleost fish. J. Immunol. *184*, 2355–2368.

Robertson, A.L., Holmes, G.R., Bojarczuk, A.N., Burgon, J., Loynes, C.A., Chimen, M., Sawtell, A.K., Hamza, B., Willson, J., Walmsley, S.R., et al. (2014). A zebrafish compound screen reveals modulation of neutrophil reverse migration as an anti-inflammatory mechanism. Sci Transl Med *6*, 225ra29.

Roca, F.J., Mulero, I., López-Muñoz, A., Sepulcre, M.P., Renshaw, S.A., Meseguer, J., and Mulero, V. (2008). Evolution of the inflammatory response in vertebrates: fish TNF-alpha is a powerful activator of endothelial cells but hardly activates phagocytes. J. Immunol. *181*, 5071–5081.

Rock, K.L., Latz, E., Ontiveros, F., and Kono, H. (2010). The sterile inflammatory response. Annu. Rev. Immunol. *28*, 321–342.

Roelofs, M.F., Boelens, W.C., Joosten, L.A.B., Abdollahi-Roodsaz, S., Geurts, J., Wunderink, L.U., Schreurs, B.W., van den Berg, W.B., and Radstake, T.R.D.J. (2006). Identification of small heat shock protein B8 (HSP22) as a novel TLR4 ligand and potential involvement in the pathogenesis of rheumatoid arthritis. J. Immunol. *176*, 7021–7027.

Ruipérez, V., Astudillo, A.M., Balboa, M.A., and Balsinde, J. (2009). Coordinate regulation of TLR-mediated arachidonic acid mobilization in macrophages by group IVA and group V phospholipase A2s. J. Immunol. *182*, 3877–3883.

Sandri, S., Rodriguez, D., Gomes, E., Monteiro, H.P., Russo, M., and Campa, A. (2008). Is serum amyloid A an endogenous TLR4 agonist? J. Leukoc. Biol. *83*, 1174–1180.

Van der Sar, A.M., Stockhammer, O.W., van der Laan, C., Spaink, H.P., Bitter, W., and Meijer, A.H. (2006). MyD88 innate immune function in a zebrafish embryo infection model. Infect. Immun. *74*, 2436–2441.

Sato, S., Sugiyama, M., Yamamoto, M., Watanabe, Y., Kawai, T., Takeda, K., and Akira, S. (2003). Toll/IL-1 receptor domain-containing adaptor inducing IFN-beta (TRIF) associates with TNF receptor-associated factor 6 and TANK-binding kinase 1, and activates two distinct transcription factors, NF-kappa B and IFN-regulatory factor-3, in the Toll-like receptor signaling. J. Immunol. *171*, 4304–4310.

Satta, N., Dunoyer-Geindre, S., Reber, G., Fish, R.J., Boehlen, F., Kruithof, E.K.O., and de Moerloose, P. (2007). The role of TLR2 in the inflammatory activation of mouse fibroblasts by human antiphospholipid antibodies. Blood *109*, 1507–1514.

Sbalzarini, I.F., and Koumoutsakos, P. (2005). Feature point tracking and trajectory analysis for video imaging in cell biology. J. Struct. Biol. *151*, 182–195.

Schaefer, L., Babelova, A., Kiss, E., Hausser, H.-J., Baliova, M., Krzyzankova, M., Marsche, G., Young, M.F., Mihalik, D., Götte, M., et al. (2005). The matrix component biglycan is proinflammatory and signals through Toll-like receptors 4 and 2 in macrophages. J. Clin. Invest. *115*, 2223–2233.

Schaeffler, A., Gross, P., Buettner, R., Bollheimer, C., Buechler, C., Neumeier, M., Kopp, A., Schoelmerich, J., and Falk, W. (2009). Fatty acid-induced induction of Toll-like receptor-4/nuclear factor-kappaB pathway in adipocytes links nutritional signalling with innate immunity. Immunology *126*, 233–245.

Schievella, A.R., Regier, M.K., Smith, W.L., and Lin, L.L. (1995). Calcium-mediated translocation of cytosolic phospholipase A2 to the nuclear envelope and endoplasmic reticulum. J. Biol. Chem. *270*, 30749–30754.

Schiffmann, E., Corcoran, B.A., and Wahl, S.M. (1975). N-formylmethionyl peptides as chemoattractants for leucocytes. Proc. Natl. Acad. Sci. USA *72*, 1059–1062.

Schindelin, J., Arganda-Carreras, I., Frise, E., Kaynig, V., Longair, M., Pietzsch, T., Preibisch, S., Rueden, C., Saalfeld, S., Schmid, B., et al. (2012). Fiji: an open-source platform for biological-image analysis. Nat. Methods *9*, 676–682.

Schofield, Z.V., Woodruff, T.M., Halai, R., Wu, M.C.-L., and Cooper, M.A. (2013). Neutrophils--a key component of ischemia-reperfusion injury. Shock *40*, 463–470.

Schwandner, R., Dziarski, R., Wesche, H., Rothe, M., and Kirschning, C.J. (1999). Peptidoglycan- and lipoteichoic acid-induced cell activation is mediated by toll-like receptor 2. J. Biol. Chem. *274*, 17406–17409.

Sepulcre, M.P., Alcaraz-Pérez, F., López-Muñoz, A., Roca, F.J., Meseguer, J., Cayuela, M.L., and Mulero, V. (2009). Evolution of lipopolysaccharide (LPS) recognition and signaling: fish TLR4 does not recognize LPS and negatively regulates NF-kappaB activation. J. Immunol. *182*, 1836–1845.

Serhan, C.N. (2007). Resolution phase of inflammation: novel endogenous anti-inflammatory and proresolving lipid mediators and pathways. Annu. Rev. Immunol. *25*, 101–137.

Serhan, C.N., and Savill, J. (2005). Resolution of inflammation: the beginning programs the end. Nat. Immunol. *6*, 1191–1197.

Sharma, S., tenOever, B.R., Grandvaux, N., Zhou, G.-P., Lin, R., and Hiscott, J. (2003). Triggering the interferon antiviral response through an IKK-related pathway. Science (80-.). *300*, 1148–1151.

Shi, H., Kokoeva, M.V., Inouye, K., Tzameli, I., Yin, H., and Flier, J.S. (2006). TLR4 links innate immunity and fatty acid-induced insulin resistance. J. Clin. Invest. *116*, 3015–3025.

Shi, J., Zhao, Y., Wang, Y., Gao, W., Ding, J., Li, P., Hu, L., and Shao, F. (2014). Inflammatory caspases are innate immune receptors for intracellular LPS. Nature *514*, 187–192.

Simpson, D.M., and Ross, R. (1972). The neutrophilic leukocyte in wound repair a study with antineutrophil serum. J. Clin. Invest. *51*, 2009–2023.

Starnes, T.W., and Huttenlocher, A. (2012). Neutrophil reverse migration becomes transparent with zebrafish. Adv Hematol *2012*, 398640.

Stein, C., Caccamo, M., Laird, G., and Leptin, M. (2007). Conservation and divergence of gene families encoding components of innate immune response systems in zebrafish. Genome Biol. *8*, R251.

Stockhammer, O.W., Zakrzewska, A., Hegedûs, Z., Spaink, H.P., and Meijer, A.H. (2009). Transcriptome profiling and functional analyses of the zebrafish embryonic innate immune response to Salmonella infection. J. Immunol. *182*, 5641–5653.

Stockhammer, O.W., Rauwerda, H., Wittink, F.R., Breit, T.M., Meijer, A.H., and Spaink, H.P. (2010). Transcriptome analysis of Traf6 function in the innate immune response of zebrafish embryos. Mol. Immunol. *48*, 179–190.

Streisinger, G., Walker, C., Dower, N., Knauber, D., and Singer, F. (1981). Production of clones of homozygous diploid zebra fish (Brachydanio rerio). Nature *291*, 293–296.

Sullivan, C., Charette, J., Catchen, J., Lage, C.R., Giasson, G., Postlethwait, J.H., Millard, P.J., and Kim, C.H. (2009). The gene history of zebrafish tlr4a and tlr4b is predictive of their divergent functions. J. Immunol. *183*, 5896–5908.

Takaki, K., Cosma, C.L., Troll, M.A., and Ramakrishnan, L. (2012). An in vivo platform for rapid high-throughput antitubercular drug discovery. Cell Rep. *2*, 175–184.

Takeuchi, O., Sato, S., Horiuchi, T., Hoshino, K., Takeda, K., Dong, Z., Modlin, R.L., and Akira, S. (2002). Cutting edge: role of Toll-like receptor 1 in mediating immune response to microbial lipoproteins. J. Immunol. *169*, 10–14.

Torraca, V., Masud, S., Spaink, H.P., and Meijer, A.H. (2014). Macrophage-pathogen interactions in infectious diseases: new therapeutic insights from the zebrafish host model. Dis. Model. Mech. *7*, 785–797.

Trede, N.S., Zapata, A., and Zon, L.I. (2001). Fishing for lymphoid genes. Trends Immunol. *22*, 302–307.

Trede, N.S., Langenau, D.M., Traver, D., Look, A.T., and Zon, L.I. (2004). The use of zebrafish to understand immunity. Immunity *20*, 367–379.

Tucker, D.E., Ghosh, M., Ghomashchi, F., Loper, R., Suram, S., John, B.S., Girotti, M., Bollinger, J.G., Gelb, M.H., and Leslie, C.C. (2009). Role of phosphorylation and basic residues in the catalytic domain of cytosolic phospholipase A2alpha in regulating interfacial kinetics and binding and cellular function. J. Biol. Chem. *284*, 9596–9611.

Tulotta, C., He, S., van der Ent, W., Chen, L., Groenewoud, A., Spaink, H.P., and Snaar-Jagalska, B.E. (2016). Imaging Cancer Angiogenesis and Metastasis in a Zebrafish Embryo Model. Adv. Exp. Med. Biol. *916*, 239–263.

Underhill, D.M., Ozinsky, A., Hajjar, A.M., Stevens, A., Wilson, C.B., Bassetti, M., and Aderem, A. (1999). The Toll-like receptor 2 is recruited to macrophage phagosomes and discriminates between pathogens. Nature *401*, 811–815.

Van der Vaart, M., Spaink, H.P., and Meijer, A.H. (2012). Pathogen recognition and activation of the innate immune response in zebrafish. Adv Hematol *2012*, 159807.

Van der Vaart, M., van Soest, J.J., Spaink, H.P., and Meijer, A.H. (2013). Functional analysis of a zebrafish myd88 mutant identifies key transcriptional components of the innate immune system. Dis. Model. Mech. *6*, 841–854.

Vance, R.E. (2000). Cutting edge: cutting edge commentary: a Copernican revolution? Doubts about the danger theory. J. Immunol. *165*, 1725–1728.

Vanden Berghe, T., Linkermann, A., Jouan-Lanhouet, S., Walczak, H., and Vandenabeele, P. (2014). Regulated necrosis: the expanding network of non-apoptotic cell death pathways. Nat. Rev. Mol. Cell Biol. *15*, 135–147.

Varela, M., Dios, S., Novoa, B., and Figueras, A. (2012). Characterisation, expression and ontogeny of interleukin-6 and its receptors in zebrafish (Danio rerio). Dev. Comp. Immunol. *37*, 97–106.

Vogl, T., Tenbrock, K., Ludwig, S., Leukert, N., Ehrhardt, C., van Zoelen, M.A.D., Nacken, W., Foell, D., van der Poll, T., Sorg, C., et al. (2007). Mrp8 and Mrp14 are endogenous activators of Toll-like receptor 4, promoting lethal, endotoxin-induced shock. Nat. Med. *13*, 1042–1049.

Vojtech, L.N., Scharping, N., Woodson, J.C., and Hansen, J.D. (2012). Roles of inflammatory caspases during processing of zebrafish interleukin-1β in Francisella noatunensis infection. Infect. Immun. *80*, 2878–2885.

Vollmer, J., Tluk, S., Schmitz, C., Hamm, S., Jurk, M., Forsbach, A., Akira, S., Kelly, K.M., Reeves, W.H., Bauer, S., et al. (2005). Immune stimulation mediated by autoantigen binding sites within small nuclear RNAs involves Toll-like receptors 7 and 8. J. Exp. Med. *202*, 1575–1585.

Weiner, H.L., and Frenkel, D. (2006). Immunology and immunotherapy of Alzheimer's disease. Nat. Rev. Immunol. *6*, 404–416.

Werts, C., Tapping, R.I., Mathison, J.C., Chuang, T.H., Kravchenko, V., Saint Girons, I., Haake, D.A., Godowski, P.J., Hayashi, F., Ozinsky, A., et al. (2001). Leptospiral lipopolysaccharide activates cells through a TLR2-dependent mechanism. Nat. Immunol. *2*, 346–352.

Wheeler, D.S., Chase, M.A., Senft, A.P., Poynter, S.E., Wong, H.R., and Page, K. (2009). Extracellular Hsp72, an endogenous DAMP, is released by virally infected airway epithelial cells and activates neutrophils via Toll-like receptor (TLR)-4. Respir. Res. *10*, 31.

White, R.M., Sessa, A., Burke, C., Bowman, T., LeBlanc, J., Ceol, C., Bourque, C., Dovey, M., Goessling, W., Burns, C.E., et al. (2008). Transparent adult zebrafish as a tool for in vivo transplantation analysis. Cell Stem Cell *2*, 183–189.

Willett, C.E., Cortes, A., Zuasti, A., and Zapata, A.G. (1999). Early hematopoiesis and developing lymphoid organs in the zebrafish. Dev. Dyn. *214*, 323–336.

Wittmann, C., Reischl, M., Shah, A.H., Kronfuss, E., Mikut, R., Liebel, U., and Grabher, C. (2015). A Zebrafish Drug-Repurposing Screen Reveals sGC-Dependent and sGC-Independent Pro-Inflammatory Activities of Nitric Oxide. PLoS One *10*, e0137286.

Wright, H.L., Moots, R.J., Bucknall, R.C., and Edwards, S.W. (2010). Neutrophil function in inflammation and inflammatory diseases. Rheumatology (Oxford). *49*, 1618–1631.

Wu, X.M., Hu, Y.W., Xue, N.N., Ren, S.S., Chen, S.N., Nie, P., and Chang, M.X. (2017). Role of zebrafish NLRC5 in antiviral response and transcriptional regulation of MHC related genes. Dev. Comp. Immunol. *68*, 58–68.

Yoo, S.K., Starnes, T.W., Deng, Q., and Huttenlocher, A. (2011). Lyn is a redox sensor that mediates leukocyte wound attraction in vivo. Nature *480*, 109–112.

Zhang, D.-C., Shao, Y.-Q., Huang, Y.-Q., and Jiang, S.-G. (2005). Cloning, characterization and expression analysis of interleukin-10 from the zebrafish (Danio rerion). J. Biochem. Mol. Biol. *38*, 571–576.

Zhu, X., Jacobs, B., Boetticher, E., Myou, S., Meliton, A., Sano, H., Lambertino, A.T., Muñoz, N.M., and Leff, A.R. (2002). IL‐5‐induced integrin adhesion of human eosinophils caused by ERK1/2‐mediated activation of cPLA2. J. Leukoc. Biol.

Ellett, F., Pase, L., H*ayman*, J.W., Andrianopoulos, A., and Lieschke, G.J. (2011). mpeg1 promoter transgenes direct macrophage-lineage expression in zebrafish. Blood 1*17*, e49–56.

Engström, P.G., Steijger, T., Sipos, B., Grant, G.R., Kahles, A., Rätsch, G., Goldman, N., Hubbard, T.J., Harrow, J., Guigó, R., et al. (2013). Systematic evaluation of spliced alignment programs for RNA-seq data. Nat. Methods 10, 1185–1191.

Enyedi, B., and Niethammer, P. (2017). Nuclear membrane stretch and its role in mechanotransduction. Nucleus 8, 156–161.

Enyedi, B., Kala, S., Nikolich-Zugich, T., and Niethammer, P. (2013). Tissue damage detection by osmotic surveillance. Nat. Cell Biol. *15*, 1123–1130.

Enyedi, B., Jelcic, M., and Niethammer, P. (2016). The Cell Nucleus Serves as a Mechanotransducer of Tissue Damage-Induced Inflammation. Cell 1*65*, 1160–1170.

Feinbaum, R.L., Urbach, J.M., Liberati, N.T., Djonovic, S., Adonizio, A., Carvunis, A.-R., and Ausubel, F.M. (2012). Genome-wide identification of Pseudomonas aeruginosa virulence-related genes using a Caenorhabditis elegans infection model. PLoS Pathog. 8, e1002813.

Feng, Y., and Martin, P. (2015). Imaging innate immune responses at tumour initiation: new insights from fish and flies. Nat. Rev. Cancer 1*5*, 556–562.

Finck-Barbançon, V., Goranson, J., Zhu, L., Sawa, T., Wiener-Kronish, J.P., Fleiszig, S.M., Wu, C., Mende-Mueller, L., and Frank, D.W. (1997). ExoU expression by Pseudomonas aeruginosa correlates with acute cytotoxicity and epithelial injury. Mol. Microbiol. *25*, 547–557.

Fitsialos, G., Chassot, A.-A., Turchi, L., Dayem, M.A., LeBrigand, K., Moreilhon, C., Meneguzzi, G., Buscà, R., Mari, B., Barbry, P., et al. (2007). Transcriptional signature of epidermal keratinocytes subjected to in vitro scratch wounding reveals selective roles for ERK1/2, p38, and phosphatidylinositol 3-kinase signaling pathways. J. Biol. Chem. *282*, 15090–15102.

Fitzpatrick, F.A., and Soberman, R. (2001). Regulated formation of eicosanoids. J. Clin. Invest. *107*, 1347–1351.